Active tactile exploration and tactually induced turning in tethered walking stick insects

Volker Berendes[1,*], Volker Dürr[1,2]

[1] Biological Cybernetics, Faculty of Biology, Bielefeld University, Bielefeld, Germany

[2] Center for Cognitive Interaction Technology, Bielefeld University, Bielefeld, Germany

[*] Corresponding author

Email addresses: volker.berendes@uni-bielefeld.de; volker.duerr@uni-bielefeld.de

Keywords: insect antenna, tactile sensing, tactile sampling, heading, exploration

Acknowledgements

We thank Florian P. Schmidt for his technical support and solutions for several electronic issues concerning the synchronization of multiple camera types, position sensors and linear robot. Florian Hofmann and Marco Schultz built the linear robot and Dr. Hansjürgen Dahmen (University of Tübingen) fabricated the light-weight sphere and the trackball recording hardware. VB thanks Roberta Anna Iseppi for help with a mathematical problem at an early stage of the project.

Abstract

Many animals use their tactile sense for active exploration and tactually guided behaviors like near-range orientation. In insects, tactile sensing is often intimately linked to locomotion, resulting in the orchestration of several concurrent active movements, including turning of the entire body, rotation of the head, and searching or sampling movements of the antennae. The present study aims at linking the sequence of tactile contact events to associated changes of all three kinds of these active movements (body, head and antennae). To do so, we chose the Indian stick insect *Carausius morosus*, a common organism to study sensory control of locomotion. Methodologically, we combined recordings of walking speed, heading, whole-body kinematics and antennal contact sequences during stationary, tethered walking and controlled presentation of an “artificial twig” for tactile exploration.

Our results show that object presentation episodes as brief as five seconds are sufficient to allow for a systematic investigation of tactually-induced turning behavior in walking stick insects. Animals began antennating the artificial twig within 0.5 s. and altered the beating-fields of both antennae in a position-dependent manner. This change was mainly carried by a systematic shift of the head-scape joint movement and accompanied by associated changes in contact likelihood, contact location and sampling direction of the antennae. The turning tendency of the insect also depended on stimulus position, whereas the active, rhythmic head rotation remained un-affected by stimulus presentation.

We conclude that the azimuth of contact location is a key parameter of active tactile exploration and tactually-induced turning in stick insects.

Introduction

When animals navigate through the world they use all of their senses to acquire information about their environment in order to find food and potential mating partners, or to detect danger. Other than vision or hearing, the sense of touch requires physical interaction of the sensory organ with an object or surface. As a consequence, tactile cues are literally within reach, thus providing immediate and reliable near-range formation for course control (e.g., Cowan et al., 2006) and way finding (e.g., (Ritzmann et al., 2012) during locomotion in both mammals (Grant et al., 2018) and arthropods (Staudacher et al., 2005). Although the sensory organs are very different in mammals (vibrissae) and insects (antennae), many representatives of both taxa rhythmically move their tactile sensors for active tactile sampling of the ambient space (Prescott et al., 2011). For example, rats and mice rapidly sweep their whiskers back and forth in order to localize objects (e.g., Ahissar and Knutsen, 2008; Mitchinson et al., 2007) and arthropods like crayfish (Zeil et al., 1985), cockroaches (Okada and Toh, 2004) and stick insects (Dürr et al., 2001a) actively move their antennae when navigating their habitats. Since cockroaches and stick insects are important study organisms in locomotion research, the role of their long antennae in motor flexibility is particularly intriguing (Dürr et al., 2018). As crepuscular or nocturnal species, cockroaches and stick insects make use of their tactile sense during walking (Okada and Toh, 2001, 2006), running (Camhi and Johnson, 1999; Cowan et al., 2006; Mongeau et al., 2013), obstacle negotiation (Harley et al., 2009; Krause and Dürr, 2012)and climbing (Schütz and Dürr, 2011).

Additionally to the temporal and spatial coordination of the walking legs, most, if not all of these locomotor behaviors involve simultaneous control of head and antennal movements. While the whisker system of rodents has been studied in great detail on both behavioral and neuronal levels (Adibi, 2019), including the detailed coordination of whisking, sniffing and head movement (e.g., (Kurnikova et al., 2017), we still have quite limited understanding of similar coordination between antennae, head and leg movement in insects. Although pionieering studies on stationary walking cockroaches have revealed context-dependent changes in antennal movement pattern (Okada and Toh, 2004) and the relationship between antennal contact frequency and turning (Okada and Toh, 2006), it remains unclear how the two antennal joints contribute to tactile sampling, and how much head movement is involved. Similarly, important first insights into the neural correlates of tactually induced turning behavior in cockroaches (Guo and Ritzmann, 2013) need to be complemented by a more detailed understanding of the complex coordination of the active sampling process.

Here, we take a first step into this direction by using tethered walking stick insects that, owing to their relatively large, protruding head and kinematic constraints of their antennal base (Krause and Dürr, 2004) allow combined recording of head, antenna and leg movements as the animals probe and respond to a tactile stimulus. To do so, we combine high-precision motion capture (e.g. Theunissen and Dürr, 2013) and path reconstruction on a trackball setup (e.g. Dahmen et al., 2017; Seelig et al., 2010; Buchner, 1976) with automated stimulus presentation. Given the spatial and temporal complexity of the active antennal movement pattern (Krause and Dürr, 2012; Krause et al., 2013) and tactually induced reaching movements (Schütz and Dürr, 2011) of stick insects, it is very challenging if not impossible to control the properties of tactile contact events in unrestrained walking animals. Accordingly, the rationale of our approach is to apply brief episodes of tactile stimulus presentation to tethered walking animals, thus narrowing down the variation of contact event properties such as direction, distance and contact number so as to relate behavioral response variables such as turning tendency, head yaw, and antennal joint angles to contact location. Since Schütz and Dürr (2011) found a weak but significant change in body yaw angle towards a vertical rod, the first hypothesis of our study is that stick insects, like cockroaches (Okada and Toh, 2006), turn towards a tactile contact site in an azimuth-dependent manner. To test this, we present an "artificial twig" within the distal third of the antennal working range, where stick insects typically contact obstacles for the first time during walking (Dürr and Schilling, 2018). Given the slanted, orthogonal antennal joint axes of the stick insect antenna (Krause and Dürr, 2004; Mujagic et al., 2007), we further expect to find systematic changes in both antennal joint angles as a function of stimulus azimuth. Finally, we test for a stimulus-dependent change in active head movements during tactile exploration. We show that the overall turning response, the movement range and tactile sampling pattern of the antennae, but not the head movement depend on the azimuth the tactile stimulus.

Material and Methods

Animals

We used adult female stick insects of the species *Carausius morosus* (de Sinéty, 1901) for the experiments. Animals were obtained from the laboratory colony of Bielefeld University, where they were raised on blackberry leaves, ivy and china cabbage in a 12:12 h light/dark cycle at 22 to 24 °C.

The mean ± s.d. size of adult females in our colony is 77.2 ± 2.2 mm.

Motion capture and kinematics

Kinematic analyses were done by means of marker-based motion capture of tethered walking stick insects, using a Vicon MX system (Vicon, Oxford, UK) with four Vicon MX 10 S cameras with 25 mm F1.4 lenses and four Vicon Vero v2.2 cameras with 6.5-15.5 mm F1.7 zoom lenses. All cameras had inbuilt infrared flash lights. Focal lengths were chosen to achieve high spatial resolution in the relatively small capture volume needed for experiments on insects. The Vero cameras were connected via a Level One 16 port POE-switch (Digital Data Communications GmbH, Dortmund, Germany) and integrated in a mixed setup together with the MX 10 S cameras by means of an MX Giganet node (Vicon, Oxford, UK). The Vicon system operated at 200 frames per second, fps. An additional control video was recorded simultaneously at 50 fps, using a Basler acA1300-60gmNIR digital video camera (Basler, Ahrensburg, Germany), equipped with a 25 mm F1.4 C-mount lens (Pentax Ricoh Imaging Company Ltd., Tokyo, Japan). Data recording and post-processing was done with Nexus 2.8.1 software (Vicon, Oxford, UK).

The prothorax, legs, head and antennae of the animals were labelled with a set of ten spherical, retroreflective markers (Prophysics AG, Kloten, Switzerland) of 1.5 mm diameter and a mass of 4 mg. Markers were glued to the cuticle with transparent nail polish at the locations depicted in Fig. 1**B**. Three markers were placed on the prothorax to define a body-fixed coordinate system. The other seven markers were used to determine head orientation and limb postures. They were placed on the head, one on the proximal flagellum of either antenna, on the distal femur and distal tibia of each front leg. Three additional markers were applied to frame the treadmill, in order to establish a setup-fixed reference coordinate system. Further two markers labelled the position of the optical mouse sensors of the trackball system. Moreover, the upper and lower end of the rod (tactile stimulus, see below) were marked by a ring of retroreflective tape (Scotchlite™ M3SS-28 8850, 3M Corp., St. Paul/MN, USA).

The accuracy of the obtained marker trajectories was approx. 0.2 mm in 3D space. Kinematics of the head, prothorax, front leg and antennae were calculated from 3D marker trajectories by use of a custom-written MATLAB toolbox, as described by Theunissen and Dürr (2013). Antennal joint angles were calculated from the estimated pointing direction of the flagellum, using the inverse kinematics described by Krause and Dürr (2004).

Spherical treadmill and presentation of tactile stimulus

The animals walked on the vertex of an air-cushioned, spherical treadmill of 20 cm diameter (Fig. 1A) very much like the treadmill used by Ebeling and Dürr (2005). The treadmill allowed registration of three degrees of freedom of the animal's movement, i.e., forward and sideward translation, and yaw rotation. The light-weight (6 g), hollow Styrofoam sphere was manufactured by Dr. H.-J. Dahmen, University of Tübingen. Owing to the rotational inertia of the sphere, animals had to generate substantially larger torques for yaw rotation than if rotating their own body only. As yet, earlier studies on visually induced curve walking on a sphere with the same rotational intertia showed that stick insects can easily generate the torques required for fast and very tight yaw turns (Ebeling and Dürr, 2005). Yaw, pitch and roll movement of the sphere was recorded by integrating movement signals from two optical mouse sensors (ADNS-3050, Avago Technologies, San Jose,CA, USA), using the same basic hardware as described by Dahmen et al. (2017). The hard- and software of the tracking system was modified such that data recording could be triggered and synchronized by means of a rectangular pulsed frame trigger signal delivered by the Vicon MX system. A custom-written Matlab GUI allowed us to calculate the walking trajectory of the animals from the movement of the sphere, using the method described by Seelig et al. (2010).

Throughout this study, the tactile stimulus consisted of a vertical metal rod of 3 mm diameter that was positioned in the working-range of the antennae. This was half the diameter of the rod used by Schütz and Dürr (2011) because the objective of this present study was to constrain antennal azimuth during contact events while ensuring a robust behavioral response. For controlled stimulus presentation we used a custom-built, two-axis, linear robot that actuated a platform on which the rod was mounted to a magnetic base. Each axis of the robot consisted of a leadscrew that was turned by a NEMA 17 stepper motor with 100 steps per mm (1.8 °/step on a 2 mm thread). Maximum machine speed along each axis was set to 25 mm s^{-1}. The robot was controlled by a custom-written Matlab GUI that sent g-code positioning commands to an Arduino microcontroller (Arduino UNO R3, https://www.arduino.cc/) running the open-source software Grbl v.1.1 (https://github.com/grbl/). The stepper motors were driven by an Arduino CNC motor shield v3 equipped with DRV8825 motor drivers (Texas Instruments Inc., Dallas/TX, USA) and an external switching power supply (19.5 V, 3.3 A, Dell, Round Rock/TA, USA).

Experimental procedure

In order to avoid visual biases of active exploration behavior, animals were blindfolded prior to the experiment by covering both compound eyes with black acrylic paint. The animals were then tethered below a plastic cable tie (material PA 6.6, width 3.3 mm, thickness 1.2 mm, lever from

attachment point 84.3 mm) with black tape. The flexibility of the cable tie for lift and pitch ensured that animals could adjust their clearance and carried their own body weight. At the same time, the sideward stiffness of the cable tie prevented yaw rotation of the body axis. Walking sequences either started spontaneously or were induced by touching the abdomen with a fine paint brush. Following an episode of walking without external stimuli, a tactile stimulus was presented by moving the vertical rod into the distal third of the working range of the antennae (Fig. 1C). The rod was then held stationary for 5 s, before it was moved back out of the antennal working range. For offline data analysis, each trial was later divided into two episodes of 5 s duration: a control episode prior to antennal contact, and a test episode with antennal contacts. To avoid habituation effects or position learning, the stimulus positon, i.e., the angular position (azimuth) of the rod with regard to the head of the animal, was drawn pseudo-randomly, trial-by-trial from a set of 9 locations (Fig. 1C). The exact angular position of the stimulus was calculated later from the motion capture data.

Data analysis

All data analysis was done in MATLAB R2018a (The MathWorks, Natick, MA, USA), including some functions from shared toolboxes available from the MATLAB File Exchange (packages “Violin Plots for plotting multiple distributions” vs 1.15.0.0 by Jonas Dorn and “Shade area between two curves” vs. 1.1.0.0 by John Bockstege).

Antennal contacts with the rod were determined based on the distance of the antennal flagellum and the midline of the rod. To calculate this distance, d, we assumed that the flagellum was a straight line of the correct flagellum length, drawn from the antennal base through the antennal marker (Fig. S1). A contact event was registered whenever d was smaller than $r+\varepsilon$, where r is the radius of the rod (1.5 mm) and ε is a threshold environment of 1.7 mm around the rod (marker diameter + measurement accuracy). As the markers were attached to the dorsal surface of the flagellum, the estimated azimuth of antennal orientation was not biased by this simplification. In contrast, the elevation estimate was subject to a systematic positive bias that depended on the marker distance (Fig. S1). As a consequence, we expressed changes of antennal elevation not in absolute terms, but as changes relative to the median elevation prior to first antennal contact. Similarly, estimated contact locations on the rod were biased towards higher values (upward), however these biases did not affect any of the conclusions presented in this paper. Leg contacts with the rod were detected by the same heuristic, using a straight line through the femur-tibia joint and the distal tibia marker with the length measured during the preparation. In some figures the abbreviations AntL and AntR were used for the left- and right antenna, respectively.

Mean number of leg and antennal contacts per stimulus position were calculated from per-animal means. Bootstrapped confidence intervals were obtained from 10000 bootstrap samples. To obtain per-angle likelihood for an antenna to be in contact with the object after adduction, and likelihood of antennal elevation during contact, we divided the mean number of occurrences for a given condition (e.g., adduction of the antenna) by the sum of all means of all possible conditions. Mean frame numbers were calculated from per-animal means and separately for each stimulus position.

Heading was defined as the cumulative yaw turn angle in degrees. It was reset to zero at the instant of first antennal contact, thus yielding two values per trial: one prior to and one after antennal contact. Mean heading direction was calculated using the Circular Statistics Toolbox for Matlab (Berens and Valesco, 2009). For every stimulus position, mean heading was calculated first per animal and then for the distribution of per-animal means. The same was done for antennal azimuth and elevation angles and percentiles. Since we used a right-handed Cartesian coordinate system throughout this study, negative azimuth values for stimulus position correspond to the right-hand side of the animal. For intuitive visualization, azimuth of stimulus position was plotted on a reverse abscissa (values increase from right to left) so as to reflect real-world spatial orientation.

The “beating field” of an antenna or the head is defined as the two-dimensional projection of the respective pointing direction of the antenna or head. Beating field boundaries were determined by the 5-to-95% percentile range of either azimuth (projection on horizontal plane) or elevation (projection on sagittal plane). Density heat maps for two-dimensional histograms of antennal azimuth and elevation were calculated individually for every animal and normalized to a volume of 1. For every stimulus position, pooled data were then displayed as the sum of these normalized per-animal histograms. Similarly, histograms of vertical antennal contact locations along the rod were calculated individually for every animal. This was done by dividing the vertical size of the rod into 100 bins and counting the number of video frames during which an antenna was in contact with the medial or lateral side of the rod in a particular position. In order to provide estimates of contact distributions for an average trial, per-animal histograms were divided by the number of trials of that animal. Pooled data were described as mean normalized per-animal histograms. Knowing the onset and end times of each antennal contact event with the vertical surface of the rod, we categorised each contact event according to the antennal movement direction prior to contact (abduction or adduction) and according to movement direction during the contact event (upward or downward).

In all box-and-whisker plots, the central mark indicates the median, while bottom and top edges of the box indicate the interquartile range (IQR, i.e. from 25 % and 75 % percentiles). Whiskers show the data range, excluding outliers. Outliers were defined as data points beyond 1.5 times the IQR away from the box.

All statistical analyses on non-circular data were calculated using the Statistics and machine learning toolbox of Matlab. Only non-parametric statistical tests were used, and all tests were calculated on per-animal means or medians. Sample sizes per animal and per test are given in **Table 1**. Spearman's rank correlation coefficient was used to test whether measured variables correlated with stimulus position. For the analysis of changes in heading angle (Fig. 5 and S2), a Kruskal-Wallis test was used to test for differences among sample medians from multiple stimulus positions, followed by a posthoc analysis of pair-wise differences using a Mann-Whitney U test with Šidak adjustment for multiple comparisons.

Results

The two hypotheses to be tested by this study were that (i) stick insects turn towards a tactile contact site in an azimuth-dependent manner, and (ii) that movement of the head and both antennal joints is involved in this behavior by means of correlated, stimulus-dependent changes. To test these hypotheses, we combined whole-body motion capture and track reconstruction of tethered walking stick insects with controlled presentation of an "artificial twig". This twig was a vertical rod that served as a narrow vertical contact surface, allowing us to test for position-dependent changes in tactually induced walking and exploration behavior. In total, we conducted experiments with 25 adult, female tethered walking animals in a total of 774 experimental trials. Once an animal had walked for a few seconds, the tactile stimulus – a vertical rod – was moved into the working range of the antennae and held stationary at one of nine stimulus positions within an angular range of -40 to 40 ° relative to the body axis **(Fig. 1 A and C)**. For every trial, we determined the time at which the stimulator had moved half-way between its parking position (average distance and range from head marker: 44.6 mm [33.6, 53.1]) and the stimulus position within the antennal range (average distance and range: 30.8 mm [23.9, 43.5]). Around this time point, we searched for antennal and leg contacts with the rod. As the animals were blindfolded prior to the experiment, the only sense that could inform them about the presence of the object was touch. In 4.3 % of all trials (n = 33), the animals failed to touch the rod. In 0.5 % of all trials (n = 4) only the leg touched the rod. These trials were excluded from further analysis. In 95.2 % of all trials (n = 737), we found at least one antennal contact with the rod. Only these trials were evaluated further. Detailed numbers of animals and trials recorded per stimulus position can be found in **Table 1A**. A total of 18 animals made antennal contact in at least one trial per stimulus position.

To illustrate how the animals responded to the presentation of the tactile stimulus, Fig. 2 shows time courses of the main analysis variables for a trial with the stimulus held at an azimuth of -40 °, i.e., to the right of body axis. The time window of ±5 s is centered on the time of the first antennal contact which, in this case, occurred approx. 2.8 s after the vertical rod entered the working-range of the antennae. The grey shaded area in Fig. 2 marks the 5 s episode of stimulus presentation (see stimulus distance in Fig. 2A). Prior to the first antennal contact, the animal turned leftwards, as its heading angle increased (Fig. 2B; upon antennal contact, the heading value was reset to zero). In total, this animal touched the rod twice with its right antenna and once with its left antenna (black markings on blue and red joint angle time courses, respectively; Fig. 2D, E). After the first antennal contact, the heading (Fig. 2B) and azimuth angles of the head (Fig. 2C) and both antennae (Fig. 2D) changed to more negative values, i.e. towards the side of the stimulus. Accordingly, the azimuth of the stimulus relative to the head midline shifted towards the zero line (black dotted line in Fig. 2D). For corresponding time courses of leg joint angles (which were not used in the present analysis) and a comparison of antennal trajectories, pointing directions and joint angles of the same trial, see Suppl. Fig. S2.

Tactile exploration of the obstacle is fast and position-dependent

In order to have a within-trial comparison of animal behavior before and during tactile exploration, we set the time of the first antennal contact with the rod to zero, and devoted all further analysis to the time windows 5 s before and after this first antennal contact. Accordingly, we will refer to these two time windows as 'before and after first contact' for the rest of this text.

Animals took only about 0.5 s to detect the obstacle after its entry into the antennal working range **(Fig. 3A)**, which is well within the published range of step cycle periods in *C. morosus* (e.g.: free walking: 0.4 to 1.2 s, Graham, 1972; tethered walking: 1-2 s, Dürr and Ebeling, 2005). Once detected, the rod was repeatedly antennated, such that individual contact events were generally very short (left antenna 0.09 s; right antenna 0.12 s). In general, both antennae were able to contact the rod at all stimulus positions tested. Note that this observation includes active movement of the head. The likelihood of antennal contact depended strongly on stimulus position **(Fig. 3B)**. It was highest for stimulus positions ipsilateral to the respective antenna, averaging up to 5.5 contacts per 5 s of the left antenna at stimulus position 40 °, and up to 7 contacts per 5 s for the right antenna at -40°. Lowest contact numbers were recorded for more contralateral positions, averaging only 0.5 contacts per 5 s of the left antenna at -40 °, and 1 contact per 5 s for the right antenna at 40°. The probability that both antennae touched the rod within the same trial was highest immediately in front of the animal, i.e., at stimulus position 0 °, and declined towards more lateral stimulus positions **(Fig. 3B).**

Since the movement ranges of the front legs and antennae overlap in *Carausius morosus*, we also observed front leg contacts with the rod. This occurred in 22.6 % of all trials (n = 175; **Table 1C, Fig. 4**). Two animals showed both antennal and leg contacts in at least one trial per stimulus position. For more lateral stimulus positions (-40 to -30 °, and 20 to 40 °) a front leg occasionally touched the rod prior to the first antennal contact **(Fig. 4A)**. This was very rare (2.3 % of all trials; n = 18), and only ever occurred for the leg ispilateral to the stimulus position. In most trials with front leg contact, the animal also firmly grasped the rod with the tarsus, and sometimes this was followed by a reach-to-grasp movement by the contralateral leg, too (green bars in Fig. **4**). Owing to the tether, the animals were unable to approach the rod and climb upon it. Therefore, grasping the rod lead to the rather unphysiological situation in which an animal attempted to approach the object with fast stepping of middle and hind legs, while at least one front leg kept hold of the rod. To exclude trials with such unphysiological situations, all trials in which a leg contact was detected were discarded from the main analysis and used for a general comparison of turning tendency with and without leg contacts only (see below). In total, 72.6 % (n = 562) of all trials were included for the main analysis.

Animals turn towards the touched object

Next we wanted to know whether the presence of the rod would cause the animals to adjust their walking direction once they encountered it. As evident from Fig. 5B-D**,** the recorded walking sequences were highly variable, both in terms of walking speed and curvature. However, the trajectories in Fig. **5 B and D** suggest a tendency of the animals to turn into the direction of the stimulus. Indeed, the quantitative comparison of Fig. **5A** revealed that the mean heading after antennal contact correlated significantly with the position of the rod (Spearman's rank correlation, r_S = 0.447, $p < 0.001$), whereas is did not correlate before antennal contact (r_S = -0.078, p = 0.280). The mean heading after first antennal contact ranged from -9.3° at -40° to 13.6° at 40°. Thus, median change of heading during stimulus presentation was approximately 20 degrees per 80 degrees in stimulus position. The Kruskal-Wallis posthoc analysis also revealed significant differences between several stimulus positions **(Fig. 5Aii)**. To test whether the exclusion of leg-contact trials affected this conclusion, we repeated the same analysis with all trials (Suppl. Fig. 3). The overall result was the same as in Fig. 5: As before, there was a systematic, stimulus-dependent change in heading, though the correlation coefficient was slightly larger (r_S = 0.526, $p < 0.001$) and the details of the pair-wise tests differed slightly, too. We conclude that the exclusion of the leg-contact trials did not affect our conclusion about the position-dependency of tactually induced turning.

Antennal contact evokes position-dependent sampling of the rod

Given the tactually induced change in overall walking behavior, we wanted to know whether and how this was paralleled by position-dependent changes in active tactile exploration behavior. In a first step, we plotted the horizontal beating field, i.e., the top view projection of the working range of both antennae for all stimulus positions **(Fig. 6)**. We found a significant dependency between the position of the rod and the median pointing direction of the antennae after the first antennal contact event **(Fig. 6Aii;** Spearman's rank correlation, left: $r_s = 0.405$, $p < 0.001$, right: $r_s = 0.522$, $p < 0.001$), whereas there was no significant dependency prior to antennal contact (left: $r_s = -0.029$, $p = 0.687$; right: $r_s = -0.007$, $p = 0.923$; Fig. **6Ai)**. During the control episode before antennal contact **(Fig. 6Ai),** the horizontal beating field of the antennae had a range of approximately 70 ° (left range from 12 ° to 82 °]; right range from -76 ° to -8 °) with median pointing directions of about 30 ° for the left (ranging from 30 ° to 36 °) and -25 ° for the right antenna (ranging from -30 ° to -20 °). After the first antennal contact event **(Fig. 6Aii)** the shift of horizontal beating field followed an almost linear function with 20 ° increase for an 80 ° increase in stimulus position (left range from -2 ° to 77 °]; right range from -77 to 7 °).

Furthermore, with increasingly lateral stimulus positions we found a significant narrowing of the horizontal movement range for the antenna ipsilateral to the stimulus. This was only the case after the first antennal contact event (left: $r_s = -0.269$, $p < 0.001$; right: $r_s = 0.230$, $p < 0.001$), but not before (left: $r_s = -0.024$, $p = 0.744$; right: $r_s = 0.033$ $p = 0.648$). Since there is no evidence for a corresponding, stimulus-dependent shift of the head beating field (Spearman's rank correlation coefficient, $r_S = 0.070$, $p = 0.332$; **Fig. 6 C**), the mentioned changes in the antennal beating field were neither counteracted nor supported by active head movement.

Owing to different marker placement on the two antennae (see Suppl. Fig. S1 and corresponding text), we determined only relative changes in beating field in the vertical direction. The median antennal elevation changed significantly with rod position after the first contact had occurred (left: $r_S = 0.504$, $p < 0.001$; right: $r_S = -0.401$, $p < 0.001$), whereas there was no such dependency before (left: $r_s = 0.102$, $p = 0.159$; right: $r_s = -0.080$, $p = 0.266$). Again, the dependency was approximately linear, this time with a slope of 10 ° change in antennal elevation for an 80 ° change in stimulus position. Note that the slopes were of different sign for each antenna, as they increased with increasingly lateral stimulus positions. The range of the vertical beating field was approx. 60 ° before first antennal contact (left: -25 ° to 33 °; right: -26° to 41 °]; Fig. **6Bi)** and 60 to 70 ° after first antennal contact (left range from -30 ° to 33 °; right range from -28° to 41 °; Fig. **6Bii).**

For a more intuitive illustration of the spatial shift of the antennal beating field before and after antennal contact, Fig. 7 shows the average 2D distributions of antennal pointing directions for three stimulus conditions (For an illustration of this 2D projection of antennal tip trajectories, see Suppl. Fig. S4). As a reference mark for comparing the heat maps of Fig. 7 we fitted ellipses by eye to the top 50 % of the likelihood range of the distributions before antennal contact **(Fig. 7A)** and then copied them to the exact same positions in the distributions after antennal contact **(Fig. 7B).** Before antennal contact, the beating fields of the two antennae were separated by a central range of approx. 10 ° width. The slanted elliptic shape of each antenna's beating field corroborates the findings of Krause et al. (2013) and can be explained by the slanted, non-orthogonal arrangement of the two joint axes (Dürr et al., 2001b; Krause and Dürr, 2004; for an illustration of antennal joint axes and their relation to movement trajectories see Suppl. Fig. S2 B-D). It is due to the larger joint angle range of the head-scape joint that moves the flagellum dorso-laterally (or ventro-medially) and a narrower joint angle range of the scape-pedicel joint that moves the flagellum dorso-medially (or ventro-laterally). After antennal contact (Fig. 7B) the top 50% likelihood range shifted towards the stimulus position (azimuth +40 in Fig. 7Bi and -40 ° in Fig. 7Biii), as underscored by the mislocation of the reference ellipses. In case of the central stimulus position (azimuth 0 ° in Fig. 7Bii), there was little or no change in antennal beating field.

Note that the distributions shown in Fig. 7 are centered on the midline of the head and, therefore, do not show the antennal pointing directions within the experimental setup. This is because animals rhythmically move their head. Although the mean pointing direction and angular range of this head movement does not vary with stimulus position (Fig. 6C), it still affects the overall working range of the antennae. To illustrate this, Suppl. Fig. S4 shows the same type of graphic as in Fig. 7 but in a setup-centered coordinate system, i.e. including head movement. The main difference between these figures concerns the apparent broadening and central fusion of the left and right distributions, thus emphasising the role of the head in shaping the spatial range of active tactile exploration.

The change in antennal movement pattern is carried by the scape-pedicel joint

Since the joint axis orientation of both antennal joints of *C. morosus* is known (Krause and Dürr, 2004), we could calculate antennal joint angle time courses via inverse kinematics (for an illustration of how to relate antennal joint angle time courses to antennal tip trajectories, see Fig. S2 B-D). That way we could analyse whether both joints contributed to the contact-induced changes in antennal movement (Fig. 8). While the median head-scape (HS) joint angle of both antennae showed a positive correlation with increasingly lateral stimulus positions after (**Fig. 8 Aii**; Spearman's rank correlation; left: r_S = -0.456, $p < 0.001$; **Fig.8Bii,** right: r_S= -0.575, $p < 0.001$), but not before the first

antennal contact with the rod (**Fig.8Ai,** left: r_S = -0.027, p =0.709; **Fig.8Ai,** right: r_S= -0.004, p =0.953**)**, the effect on the scape-pedicel (SP) joint angle was inconsistent. While the SP angle of the left antenna showed no correlation with stimulus position, neither before (**Fig. 8Ci**; r_S = 0.084, p = 0.248) nor after (Fig. 8Cii; r_S = -0.068, p = 0.345) first antennal contact with the rod, the SP angle of the right antenna revealed a weak but statistically significant correlation with stimulus position after (**Fig. 8Dii**, r_S= 0.179, p =0.013) but not before contact (**Fig. 8Di**, r_S= -0.013, p =0.861). We conclude that the position-dependent change in horizontal antennal movement was predominantly carried by a systematic change of the HS joint angle.

Antennation pattern changes with stimulus position

Finally, we took a closer look at how stimulus position affected the antennation pattern of both antennae, i.e., the tactile sampling of the object. Overall, we found that the animals made more medially directed contacts with the rod, i.e., following adduction of the antenna (see red and dark blue histograms in Fig. 9A-B), than laterally directed contacts, i.e., following abduction (see magenta and light blue histograms in Fig. **9A-B)**. This was the case for both antennae and is summarized by Fig. 9C: the likelihood of antennal contacts following an adduction (medial movement) reached 1 for contralateral stimulus positions and decreased towards ipsilateral stimulus positions. For Ipsilateral contacts the likelihood of contact after adduction decreased with increasingly lateral object position, with equal likelihood for adduction and abduction around 20 °.

Generally, the antennal contact frequency was highest for ipsilateral stimulus positions and decreased towards the contralateral side of the respective antenna (Fig. 9A, B). In agreement with findings on antennal elevation (Fig. 6B), the probability of contacts on the upper half of the rod increased with increasingly lateral positions. Again this was the case for both antennae.

Antennal movement during contact events was also position-dependent (Fig. 9D, Suppl. Fig. S5). The relative frequency of upward movement along the rod (levation) was positively correlated with increasingly lateral stimulus positions in both antennae (Suppl. Fig. S5; Spearman's rank correlation; left: r_S = 0.592, p < 0.001; right: r_S = -0.686, p < 0.001). The opposite trend for downwards movements (depression) was not statistically significant (Suppl. Fig. S5; left: r_s= 0.121, p = 0.095; right: r_s = 0.090, p = 0.213).

Discussion

Other than in previous studies on tactually guided but otherwise unrestrained locomotion in stick insects (Krause and Dürr, 2012; Schütz and Dürr, 2011) the present study allowed much more precise control of tactile stimulus position, as presented to tethered, stationary walking stick insects. The main advantage of this approach was the greatly reduced variation of distance and angular position of tactile contact events, thus generating an open-loop situation with well-controlled stimulus azimuth. Since all open-loop situations entail some unnatural aspect of the animal's response, we used brief episodes of stimulus exposure, thereby limiting our results to the onset of any tactually induced change in behavior (In *C. morosus*, 5 s approximately correspond to an average of 5 step cycles). With systematic variation of stimulus azimuth within the natural working range of the stick insect antenna, our analysis focused on spatial response variables and their relation to stimulus azimuth. We found that the number of antennal contacts (Fig. 3), turning tendency (Fig. 5), antennal working range (Figs. 6, 7), mean angle of the antennal head-scape joint (Fig. 8) and antennal movement before and during contact events (Fig. 9; Fig. S5) depended significantly on stimulus azimuth. In contrast, rhythmic head movements were independent of stimulus azimuth (Fig. 6C) but added to the active exploration range of the antenna (compare Fig 7 and Fig. S4). Apart from similarities between our findings and those of similar studies on the tactile sense of other insects (Okada and Toh, 2001; 2006), there are also important differences which, at least to some extent, may be linked to differences in morphology, behavior and ecology. Moreover, our findings on tactually induced turning and antennal movement show some important differences to visually induced changes in behavior (e.g., Dürr and Ebeling, 2005). In the following we will discuss how these differences may be instructive about properties of the underlying sensorimotor circuitry.

Morphological, behavioral and ecological aspects of tactually induced turning

In stick insects, cockroaches and crickets, the typical movement pattern of the antennae during walking is a loop-like pattern that involves active movement of both antennal joints, the head-scape (HS) and the scape-pedicel (SP) joints (Dürr et al., 2001b; Horseman et al., 1997; Krause et al., 2013; Okada and Toh, 2004). Given the differences in antennal morphology between insects (reviewed by Staudacher et al., 2005) the relative contribution of the two antennal joints to this movement pattern differs greatly. In cockroaches, changes in horizontal pointing direction (antennal azimuth) are only possible by the HS joint, such that azimuth-dependent tactile responses involve sensory and motor functions of the HS joint only (Okada and Toh, 2000; 2001). In crickets, horizontal tracking movements by the antennae (Honegger, 1981) are carried by movement of the SP joint only. In stick insects, both antennal joints must act together for pure changes in antennal azimuth, because their

joint axes are slanted relative to the sagittal and horizontal planes (Mujagic et al., 2007), with the HS joint of *C. morosus* moving the antenna dorso-laterally and ventro-medially (Dürr et al., 2001). Our results show a nearly linear, position-dependent dorso-lateral shift of the median antennal pointing direction (Figs 6, 9 A, B) that is mainly carried by a systematic shift of the median HS joint angle (Fig. 8) with inconsistent and much less strong changes in median SP joint angle. We conclude that - much like in cockroaches - all tactually induced changes in behavior related to stimulus azimuth are strongly linked to sensory and motor functions of the HS joint, with little contribution of the SP joint.

Another similarity between *Periplaneta americana* and *Carausius morosus* is that both species adjust their walking direction in response to antennal tactile contact with a vertical object (Okada and Toh, 2000, 2006) in a graded, position-dependent manner. As yet, a major difference concerns the strength and persistence of this tactually-induced turning. For a stimulus position of 45 °, Okada and Toh (2000) reported a mean turning rate of 36 $°s^{-1}$ (their Fig. 7A), whereas the mean change in heading in stick insects was less than 3 $°s^{-1}$ (Fig. 5Aii). This difference can hardly be explained by different step frequencies during walking, suggesting that tactually induced turning rate per step is considerably higher in cockroaches than in stick insects. At the same time, tactually induced turning in cockroaches is a lot more persistent, with continuous turning episodes as long as 20 s (Okada and Toh, 2000; their Fig. 5) or more (Okada and Toh, 2006, their Fig. 2). Quite possibly, this difference can be explained by the fact that in *P. americana* it is possible to present a tactile stimulus within reach of an antenna but out of reach of a front leg. Since in *C. morosus* the spatial working-ranges of antennae and front legs strongly overlap (Dürr and Schilling, 2018), a vertical rod within reach of an antenna is also within reach of a front leg, too. As a consequence, long-lasting open-loop presentation of a tactile stimulus without eliciting reaching or climbing attempts is possible in cockroaches but not in stick insects.

Like turning tendency, the contact frequency per antenna was significantly dependent on the position of the rod (Figs 3, 9 A, B). However, since these dependencies are not mirrored in a correlation of contact frequency and turning tendency (Suppl. Fig. S6) we conclude that the magnitude of tactually induced turning is not a mere consequence of antennal contact number. Rather, both antennal exploration and whole-body turning must have been affected in parallel by some sensory cue about contact location. This is in contrast to experimental findings on cockroaches (Okada and Toh, 2006 their Fig. 4 and 8), where contact frequencies were similar for all stimulus positions but differences in contact frequency depended on the degree of change in running direction.

Apart from tactually induced changes in turning and antennal exploration reported in the present study, we have previously shown that stick insects respond to antennal contacts with directed reach-to-grasp movements of a front leg (Schütz and Dürr, 2011) often followed by climbing behavior (Krause and Dürr, 2012). As expected by the similar length and the fronto-lateral overlap of the spatial working ranges of antennae and front legs (Dürr and Schilling, 2018) we frequently observed reach-to-grasp movements, with more leg contacts having occurred for lateral than for medial stimulus positions (Fig. 4; Table 1). In summary, we propose that the concurrent, tactually induced changes in antennal movement, locomotion and reaching serve the function of active near-range exploration (Dürr et al., 2018) that increases the likelihood of finding foothold by a nocturnal canopy-dweller as *C. morosus*.

According to the categorization of touch-related behaviors proposed by Staudacher et al. (2005), active exploration behavior is distinct from tactually mediated course control in locomotion. The latter category is exemplified by tactually induced turning in crepuscular, domiciliary cockroaches such as *P. americana* that live in man-made environments. In *P. americana* positive thigmotaxis is strong enough to maintain tactile contact with a wall even during fast escape runs (Camhi and Johnson, 1998). Accordingly, the persistent attempt to turn toward an open-loop stimulus in cockroach locomotion may be explained by means of a PD control system reliant on contact distance (Cowan et al., 2006). In contrast, stick insects never maintain antennal contact for longer than a fraction of a step cycle, and touch-related behavior has never been found to depend on contact distance.

Differential effects of touch and vision on turning and active exploration

In free walking *C. morosus*, the antennal movement pattern is characterized by a stable phase shift between the antennal joints (Harischandra et al., 2015; Krause et al., 2013) though the overall pattern of coordination is quasi-rhythmic with variable frequency components, albeit it may appear fairly rhythmical for shorter walking episodes (Dürr et al., 2001). The tether appeared to have no effect on the antennal movement pattern, since both the horizontal (Fig. 6Ai) and vertical (Fig. 6Bi) working-ranges of both antennae before antennal contact were very similar to those described for unrestrained walking stick insects (e.g., Krause et al., 2013).

The stimulus-dependent shift of the antennal movement pattern was accompanied by repeated antennation of the vertical rod. This tactile sampling behavior involved both antennae, and the likelihood of contact events (Fig. 9A-B), the distribution of contact positions (Fig. 9A-B), the prevalent movement immediately before (Fig. 9C) and during (Fig. 9D) antennal contact event all depended on stimulus position. As animals were blindfolded, a visual contribution to the change in antennal

movement can be excluded. Instead, some of the position-dependency may be attributed to the typical antennal movement pattern during walking (e.g., Krause et al., 2013), which is characterized by an elliptic movement of the antennal tip (see Fig. S2) with an upward movement near its medial turning point, followed by abduction in the dorsal working-range, downward movement near the lateral turning point, and adduction in the ventral working range. For example, the fact that a contralateral rod is almost exclusively touched after adduction, and the position-dependent decrease of post-adduction contacts for increasingly ipsilateral stimuli (Fig. 9A-C) fits the elliptic movement pattern described above. So does our finding that increasingly ipsilateral contacts are more likely to be followed by downward movement, whereas increasingly contralateral contacts are more likely to be followed by upward movement (Fig. 9D).

The continuous antennal movement pattern in walking stick insects is superimposed on rhythmic yaw oscillations of the head (e.g., Harischandra et al., 2015; their Suppl. Fig. 3). In our case, these yaw oscillations had an approximate amplitude of ±10 ° (Fig. 6C). After antennal contact, the amplitude stayed the same, as did the median angle, rather than shifting into the walking direction. In other words, the tactually induced change in antennal beating field was not paralleled by a shift of the head beating field. This is different than in visually induced turning – the so-called optomotor response – where both the head and the antennal beating field shift into the direction of turning (Dürr and Ebeling, 2005). Also, visually induced turning is a lot stronger and more persistent than tactually-induced turning as found here. The finding that the response gain of sensory induced turning is much lower for touch than for motion vision is in line with the suggestion that our tactile stimulus primarily affected active exploration behavior rather than course control in locomotion. As yet, for both stimulus modalities stick insects tend to modulate the movement of the joint that that has the strongest effect on sensor orientation relative to the body: the neck in vision and the HS joint in touch.

Conclusion and outlook

Our data clearly show that the azimuth of antennal contact events affects the antennal movement pattern and overall turning tendency, though not the movement of the head. Despite morphological differences in their antennal motor apparatus, azimuth-dependent turning can be related to the same antennal joint in stick insects and cockroaches. Differences between tactually induced behaviors in stick insects and cockroaches may be related to (i) the different length ratio of antennae and front legs and the corresponding ability/disability to reach for antennal contact locations, but also to (ii) differences in habitat and behavioral ecology. Furthermore, differences between tactually and visually induced head movement, antenna movement and turning support the view that stick

insects use touch for spatial exploration and tactile localization within the near-range environment rather than for course control in locomotion.

While the present study focused on spatial response variables and their dependency on stimulus azimuth, future studies will need to address the effect of contact events on timing and temporal coordination of movement. In particular, the likelihood of tactually elicited reach-to-grasp movements in our tethered walking setup will allow a detailed analysis of targeted reaching behavior. Moreover, the lack of any effect of antennal contacts on head movement suggests that immobilization of the head may not affect tactually induced behavior, while allowing stable electrophysiological recordings from the head ganglia. Finally, future work will need to address how tactually induced behavior may vary with internal state and how touch is integrated with sensory cues from other modalities, including visual, wind-related or olfactory cues.

References

Adibi, M. (2019). Whisker-Mediated Touch System in Rodents: From Neuron to Behavior. *Front. Syst. Neurosci.* **13**,.

Ahissar, E. and Knutsen, P. M. (2008). Object localization with whiskers. *Biol. Cybern.* **98**, 449–58.

Berens, P. and Valesco, M. J. (2009). The Circular Statistics Toolbox for Matlab. *Tech. Rep.* 1–7.

Buchner, E. (1976). Elementary movement detectors in an insect visual system. *Biol. Cybern.* **24**, 85–101.

Camhi, J. M. and Johnson, E. N. (1999). High-frequency steering maneuvers mediated by tactile cues: antennal wall-following in the cockroach. *J. Exp. Biol.* **202**, 631–43.

Cowan, N. J., Lee, J. and Full, R. J. (2006). Task-level control of rapid wall following in the American cockroach. *J. Exp. Biol.* **209**, 1617–1629.

Dahmen, H., Wahl, V. L., Pfeffer, S. E., Mallot, H. A. and Wittlinger, M. (2017). Naturalistic path integration of *Cataglyphis* desert ants on an air-cushioned lightweight spherical treadmill. *J. Exp. Biol.* **220**, 634–644.

Dürr, V. and Ebeling, W. (2005). The behavioural transition from straight to curve walking: kinetics of leg movement parameters and the initiation of turning. *J. Exp. Biol.* **208**, 2237–2252.

Dürr, V. and Schilling, M. (2018). Transfer of Spatial Contact Information Among Limbs and the Notion of Peripersonal Space in Insects. *Front. Comput. Neurosci.* **12**, 1–20.

Dürr, V., Krause, A., Berns, K. and Dillmann, R. (2001a). The stick insect antenna as a biological paragon for an actively moved tactile probe for obstacle detection. *Proc. of CLAWAR*.

Dürr, V., Konig, Y. and Kittmann, R. (2001b). The antennal motor system of the stick insect Carausius morosus: Anatomy and antennal movement pattern during walking. *J. Comp. Physiol. A* **187**, 131–144.

Dürr, V., Theunissen, L. M., Dallmann, C. J., Hoinville, T. and Schmitz, J. (2018). Motor flexibility in insects: adaptive coordination of limbs in locomotion and near-range exploration. *Behav. Ecol. Sociobiol.* **72**, 15.

Graham, D. (1972). A behavioural analysis of the temporal organisation of walking movements in the 1st instar and adult stick insect (Carausius morosus). *J. Comp. Physiol.* **81**, 23–52.

Grant, R. A., Breakell, V. and Prescott, T. J. (2018). Whisker touch sensing guides locomotion in small, quadrupedal mammals. *Proc. R. Soc. B Biol. Sci.* **285**, 20180592.

Guo, P. and Ritzmann, R. E. (2013). Neural activity in the central complex of the cockroach brain is linked to turning behaviors. *J. Exp. Biol.* **216**, 992–1002.

Harischandra, N., Krause, A. F. and Dürr, V. (2015). Stable phase-shift despite quasi-rhythmic movements: a CPG-driven dynamic model of active tactile exploration in an insect. *Front. Comput. Neurosci.* **9**, 1–16.

Harley, C. M., English, B. A. and Ritzmann, R. E. (2009). Characterization of obstacle negotiation behaviors in the cockroach, Blaberus discoidalis. *J Exp Biol* **212**, 1463–1476.

Honegger, H. W. (1981). A preliminary note on a new optomotor response in crickets: Antennal tracking of moving targets. *J. Comp. Physiol. □ A* **142**, 419–421.

Horseman, B. G., Gebhardt, M. J. and Honegger, H. W. (1997). Involvement of the suboesophageal and thoracic ganglia in the control of antennal movements in crickets. *J. Comp. Physiol. A* **181**, 195–204.

Krause, A. F. and Dürr, V. (2004). Tactile efficiency of insect antennae with two hinge joints. *Biol. Cybern.* **91**,.

Krause, A. F. and Dürr, V. (2012). Active tactile sampling by an insect in a step-climbing paradigm. *Front. Behav. Neurosci.* **6**, 30.

Krause, A. F., Winkler, A. and Dürr, V. (2013). Central drive and proprioceptive control of antennal movements in the walking stick insect. *J. Physiol. Paris* **107**, 116–29.

Kurnikova, A., Moore, J. D., Liao, S.-M., Deschênes, M. and Kleinfeld, D. (2017). Coordination of Orofacial Motor Actions into Exploratory Behavior by Rat. *Curr. Biol.* **27**, 688–696.

Mitchinson, B., Martin, C. J., Grant, R. A. and Prescott, T. J. (2007). Feedback control in active sensing: rat exploratory whisking is modulated by environmental contact. *Proceedings. Biol. Sci.* **274**, 1035–41.

Mongeau, J. M., Demir, A., Lee, J., Cowan, N. J. and Full, R. J. (2013). Locomotion- and mechanics-mediated tactile sensing: antenna reconfiguration simplifies control during high-speed navigation in cockroaches. *J Exp Biol* **216**, 4530–4541.

Mujagic, S., Krause, A. F. and Dürr, V. (2007). Slanted joint axes of the stick insect antenna: an adaptation to tactile acuity. *Naturwissenschaften* **94**, 313–318.

Okada, J. and Toh, Y. (2000). The role of antennal hair plates in object-guided tactile orientation of the cockroach (Periplaneta americana). *J. Comp. Physiol. A* **186**, 849–857.

Okada, J. and Toh, Y. (2001). Peripheral representation of antennal orientation by the scapal hair plate of the cockroach Periplaneta americana. *J. Exp. Biol.* **204**, 4301–4309.

Okada, J. and Toh, Y. (2004). Spatio-temporal patterns of antennal movements in the searching cockroach. *J. Exp. Biol.* **207**, 3693–3706.

Okada, J. and Toh, Y. (2006). Active tactile sensing for localization of objects by the cockroach antenna. *J. Comp. Physiol. A* **192**, 715–726.

Prescott, T. J., Diamond, M. E. and Wing, A. M. (2011). Active touch sensing. *Philos. Trans. R. Soc. Lond. B. Biol. Sci.* **366**, 2989–95.

Ritzmann, R. E., Harley, C. M., Daltorio, K. A., Tietz, B. R., Pollack, A. J., Bender, J. A., Guo, P., Horomanski, A. L., Kathman, N. D., Nieuwoudt, C., et al. (2012). Deciding which way to go: how do insects alter movements to negotiate barriers? *Front Neurosci* **6**, 97.

Schütz, C. and Dürr, V. (2011). Active tactile exploration for adaptive locomotion in the stick insect. *Philos Trans R Soc L. B Biol Sci* **366**, 2996–3005.

Seelig, J. D., Chiappe, M. E., Lott, G. K., Dutta, A., Osborne, J. E., Reiser, M. B. and Jayaraman, V. (2010). Two-photon calcium imaging from head-fixed Drosophila during optomotor walking behavior. *Nat. Methods* **7**, 535–540.

Staudacher, E. M., Gebhardt, M. and Dürr, V. (2005). Antennal Movements and Mechanoreception: Neurobiology of Active Tactile Sensors.pp. 49–205.

Theunissen, L. M. and Dürr, V. (2013). Insects use two distinct classes of steps during unrestrained locomotion. *PLoS One* **8**, e85321.

Zeil, J., Sandeman, R. and Sandeman, D. (1985). Tactile localisation: the function of active antennal movements in the crayfishCherax destructor. *J. Comp. Physiol. A* **157**, 607–617.

Figures and Table

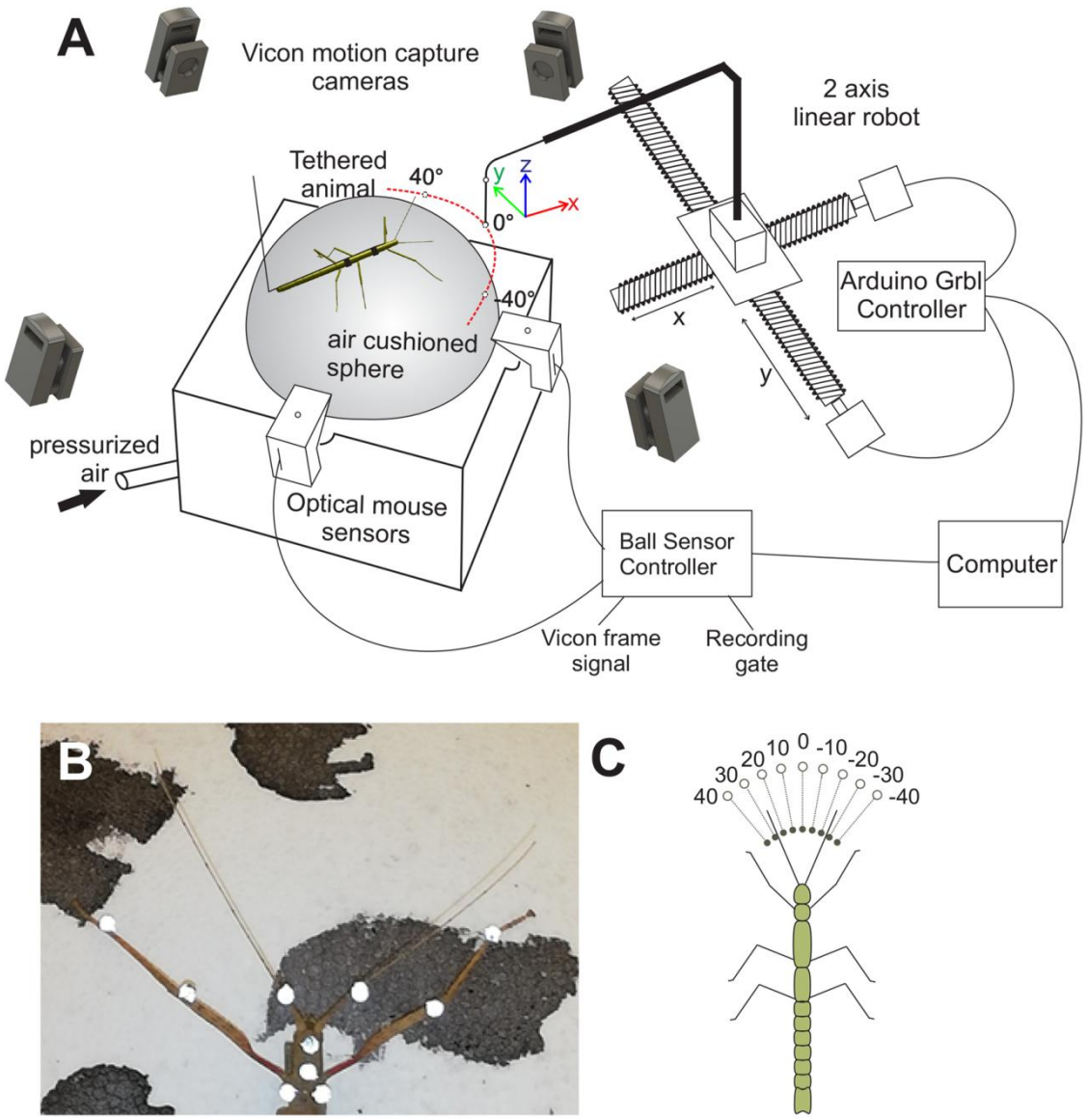

Figure 1: Experimental setup. (A) Schematic overview. Tethered stick insects were motion-captured as they walked on a spherical treadmill. A vertical metal rod served as a tactile stimulus object that was moved into the working-range of the antennae by means of a linear robot. (B) Location of 10 retroreflective, spherical markers on the animal. (C) Nine stimulus positions on a virtual semi-circle around the head of the animal before (open circles) and during presentation (filled circles). The stimulus was first positioned out of antennal reach and then introduced to the antennal range during the experiment.

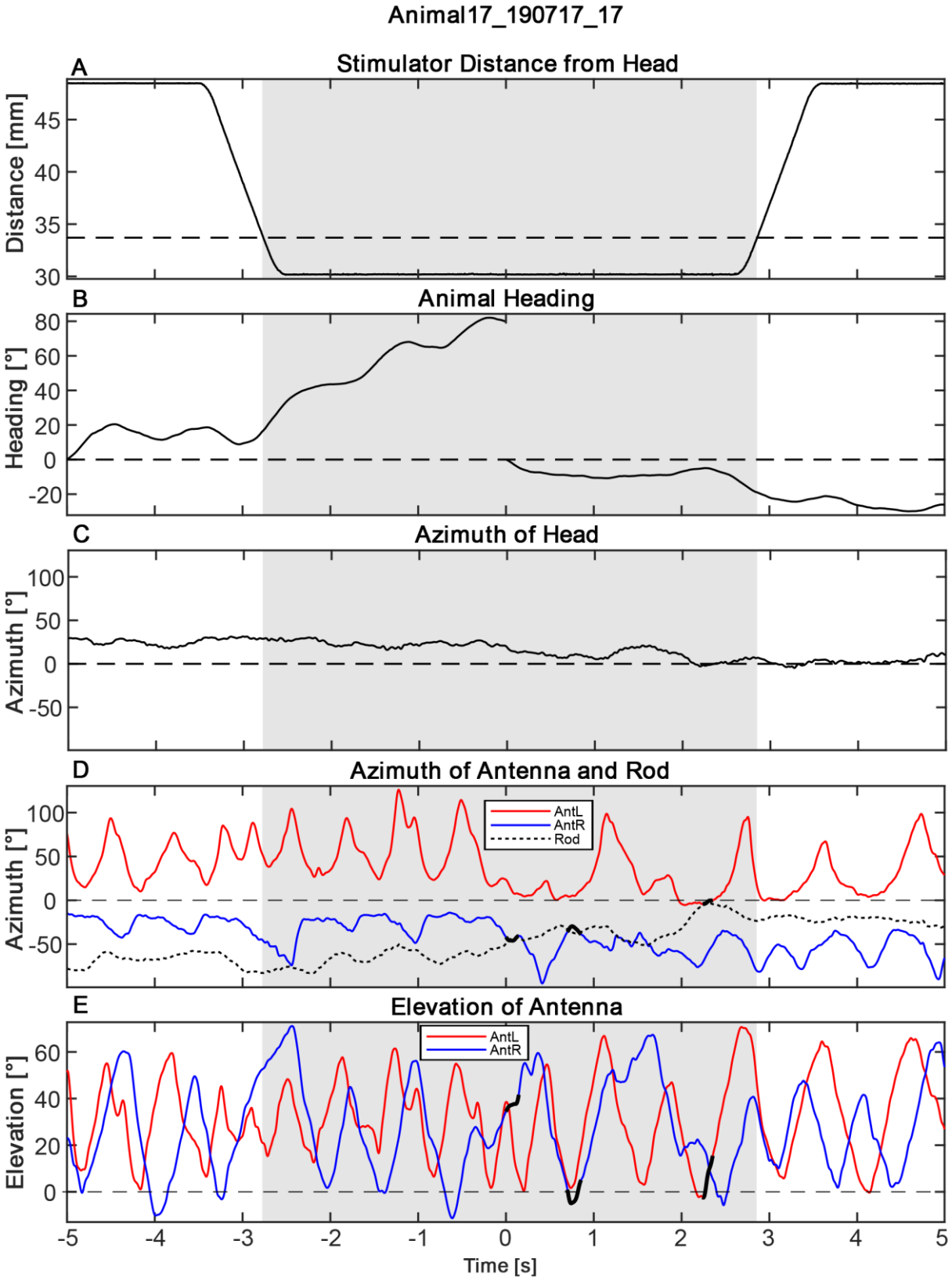

Figure 2: Time courses of heading and pointing direction of head and antennae change after first antennal contact. Synchronously recorded time courses for a 10 s time window as used for the analysis, centered on the instant of the first antennal contact with the rod (time = 0 s). From top to bottom, traces show the distance between the animal's head and the

vertical rod (A; Maximum antennal range indicated by the black dashed line), the animal's heading, i.e. cumulative turn angle (B; reset to zero at time 0), head angle within setup (C; azimuth), azimuth of antennal pointing direction and stimulus position relative to the head midline (D; red: left antenna; blue: right antenna; black: stimulus position), and elevation angle of antennal pointing direction. Three antennal contact events with the rod are marked by black overlays on the time courses of antennal pointing direction. The shaded area marks the time window during which the stimulus was within antennal range.

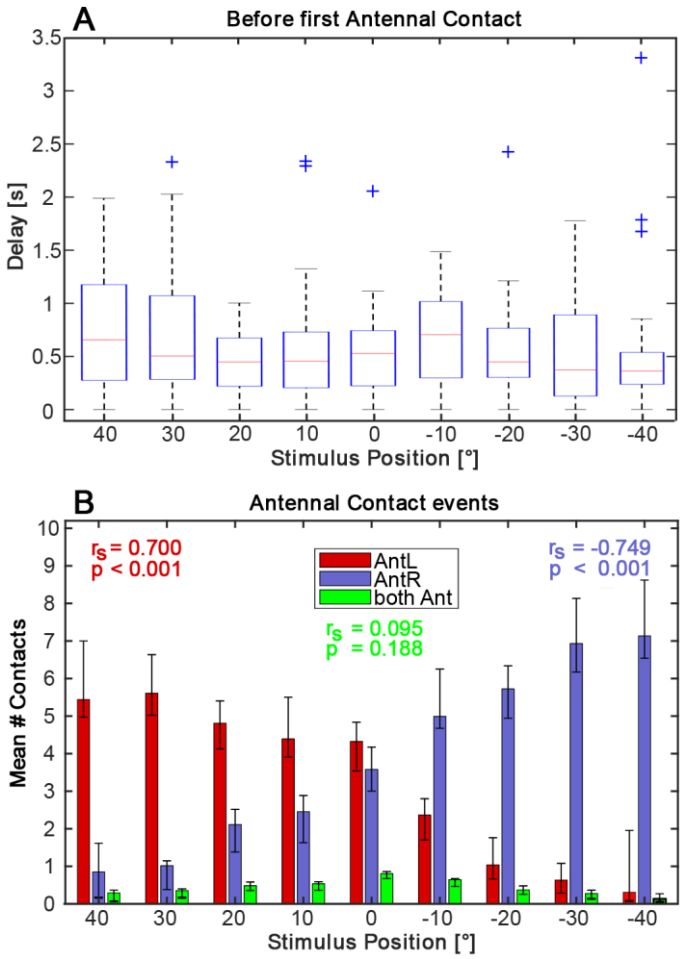

Figure *3*: Frequency of antennal contacts increases towards ipsilateral stimulus positions. (A) Mean latency of first antennal contact after the stimulus had entered the antennal range was approx. 0.5 [s]. Boxplots show per-animal means. For trial numbers, see Table 1A. (B) Mean number of antennal contacts with the rod (per trial) shown for left antenna (red), right antenna (blue) and both antennae (green; at least 1 contact of both antennae). Values are mean contact numbers per animal per trial. Error bars depict bootstrapped 95 % confidence intervals. r_s and p values refer to Spearman' rank correlation. Numbers of animals and trials in Table 1 B.

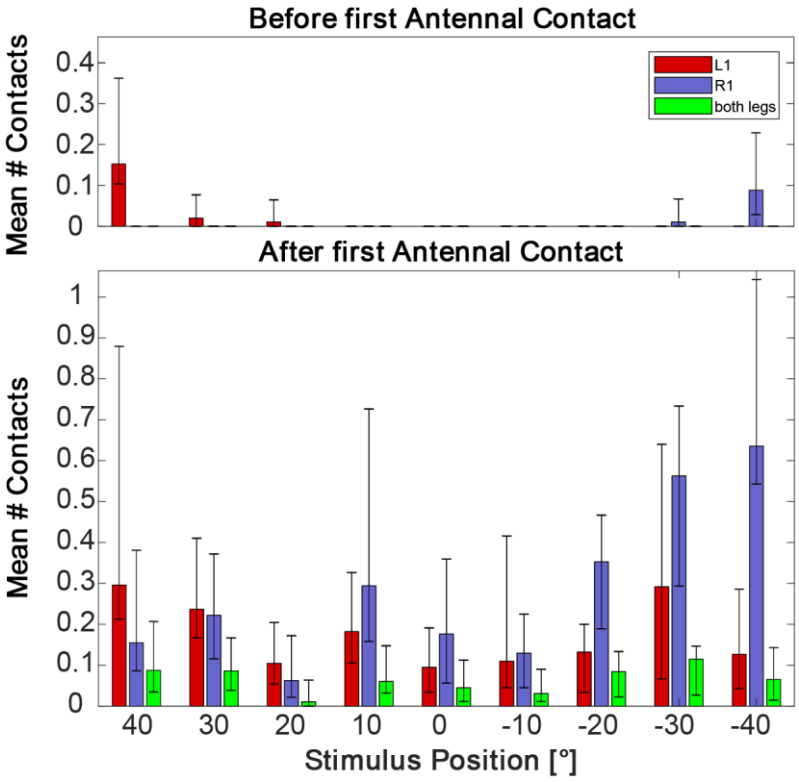

Figure *4*: Leg contacts are more likely at the margins of the antennal working range. Mean number of leg contacts with the rod (per trial) shown for left- (red) , right- (blue) and both (green) front legs before (A) and after (B) the first antennal contact event. Values are means of per-animal means. Error bars depict bootstrapped 95 % confidence intervals. Numbers of animals and trials in Table 1 C.

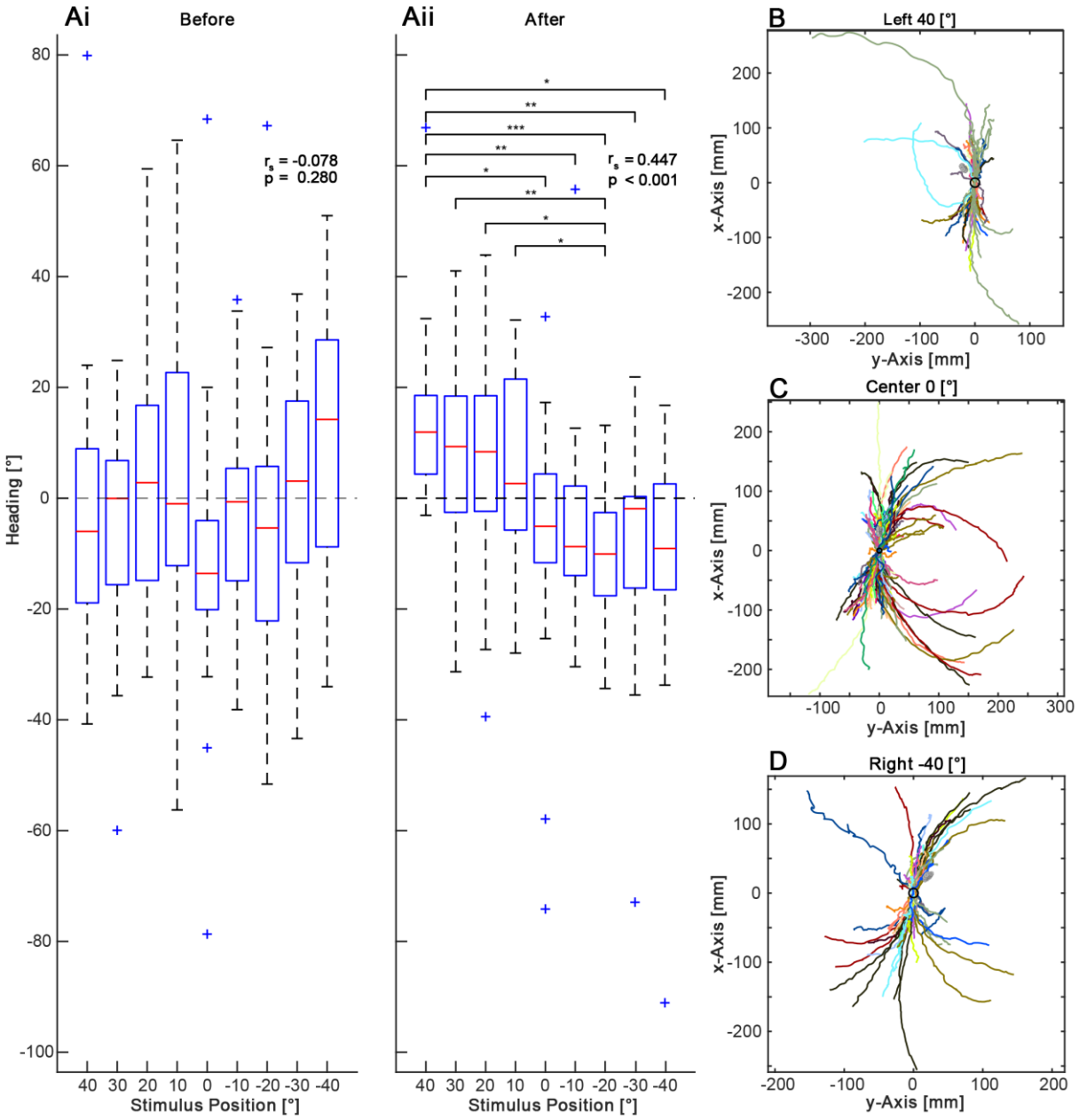

Figure *5*: Animals tend to head towards the tactile stimulus. (Ai andAii) Mean heading during walking episodes before (Ai) and after (Aii) first antennal contact with the rod. Box plots show distributions of per-animal means. Numbers of animals and trials in Table 1 B. r_S and p values correspond to Spearman's rank correlation. Pair-wise significance levels show results of a post-hoc analysis following a Kruskal-Wallis test (* $p < 0.05$; ** $p < 0.01$; *** $p < 0.001$). B-D) Animal walking trajectories, shown for all trials of the stimulus conditions -40 °, 0 ° and 40 °. Different colors indicate different animals. Trajectories were centered on the position where the first antennal contact with the rod occurred (black circle) and rotated such that their heading was 0 degrees at this position. Hence the lower and upper parts of the plots show the trajectories before and after fist antennal contact, respectively.

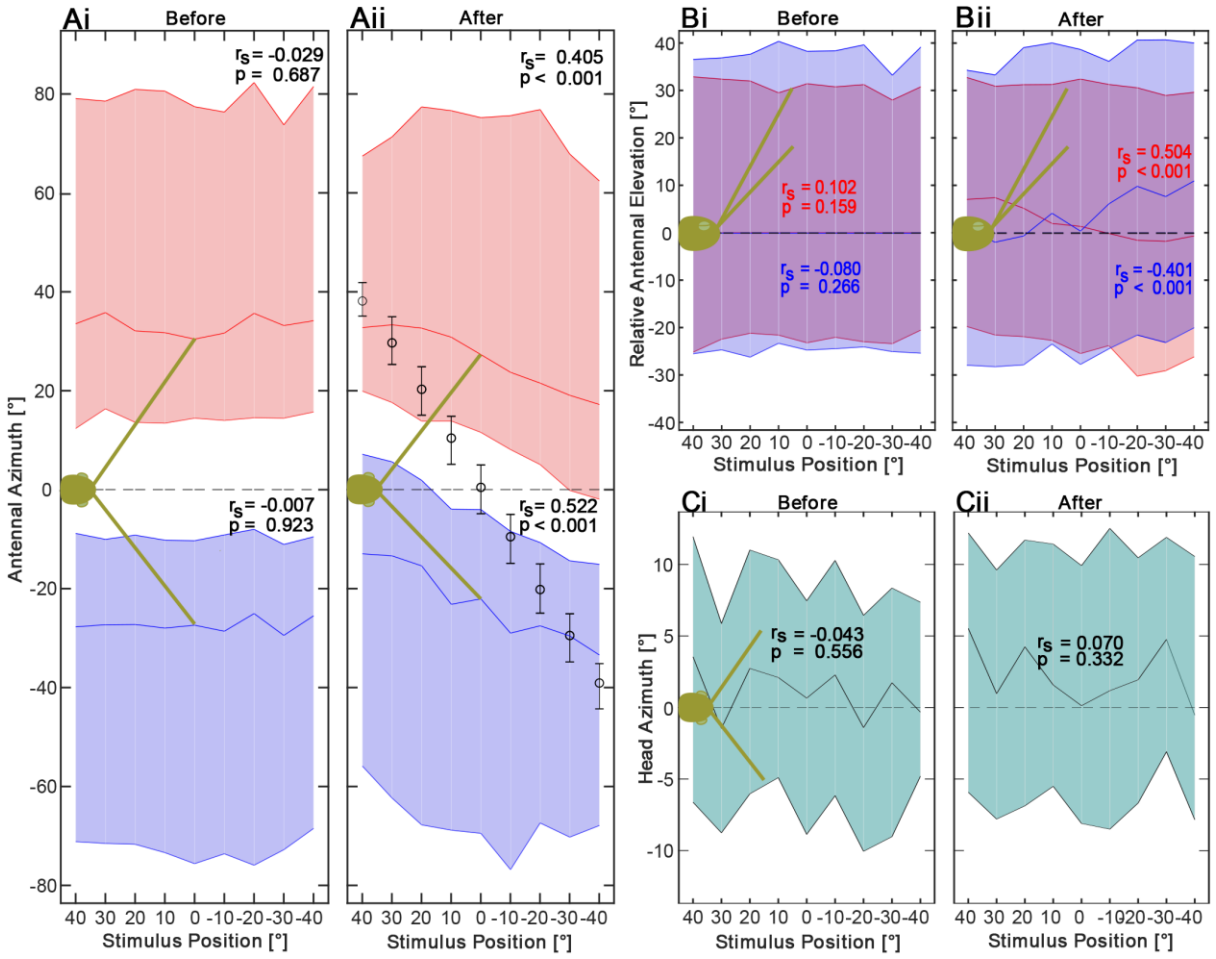

Figure *6*: Stick insects shift their antennal, but not their head beating field towards the stimulus position. *A)* The antennal beating field of the ipsilateral antenna shifts with increasingly lateral stimulus positions. Median (line) and 5-to-95% azimuthal movement range (shading) of left (red) and right (blue) antenna before (Ai) and after (Aii) first antennal contact with the rod. An azimuth of 0 corresponds to the midline of the animal's head (See insert and dashed line). Mean head-centered stimulus position (circles) and extreme values were calculated from pooled trials. B) Median (lines) and 5-to-95% range of relative elevation angles (shading) of the left (red) and right (blue) antenna before (Bi) and after (Bii) first antennal contact with the rod. Relative elevation of 0 corresponds to the median elevation angle before antennal contact (median elevation angle and range: 28.6 ° [25.3, 30.4]). Statistics were calculated on median absolute angles (not the relative angles shown in B). C) Median (line) and 5-to-95% azimuthal range (shading) of the head before (Ci) and after (Cii) first antennal contact with the rod. An azimuth of 0 corresponds to the midline of the animal's body (See insert and dashed line). In all panels, values are medians of per-animal medians, and r_S and p values give results of Spearman's rank correlation. Numbers of animals and trials in Table 1 B.

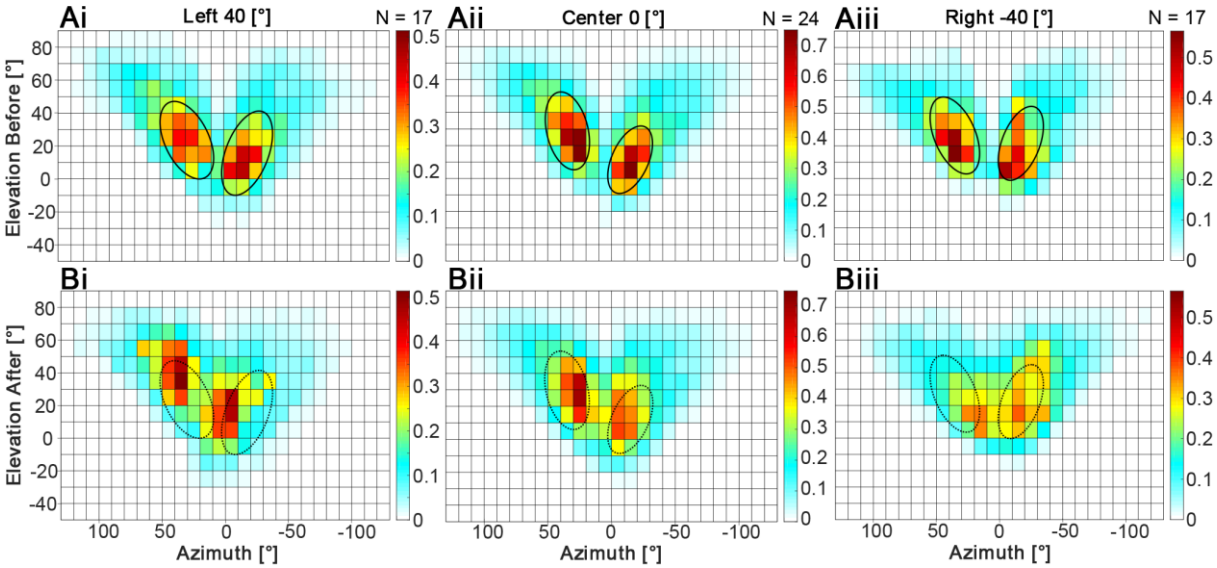

Figure *7*: Active exploration range of the antennae shifts towards stimulus location. Color-coded heat maps show antennal azimuth and elevation relative to the head in 10 ° bins before (A, top row) and after (B, bottom row) first antennal contact with the rod. Data are sums of normalized per-animal histograms with N being the number of animals. Ellipses mark the outline of the center of movement in panels A, serving as a reference in B.

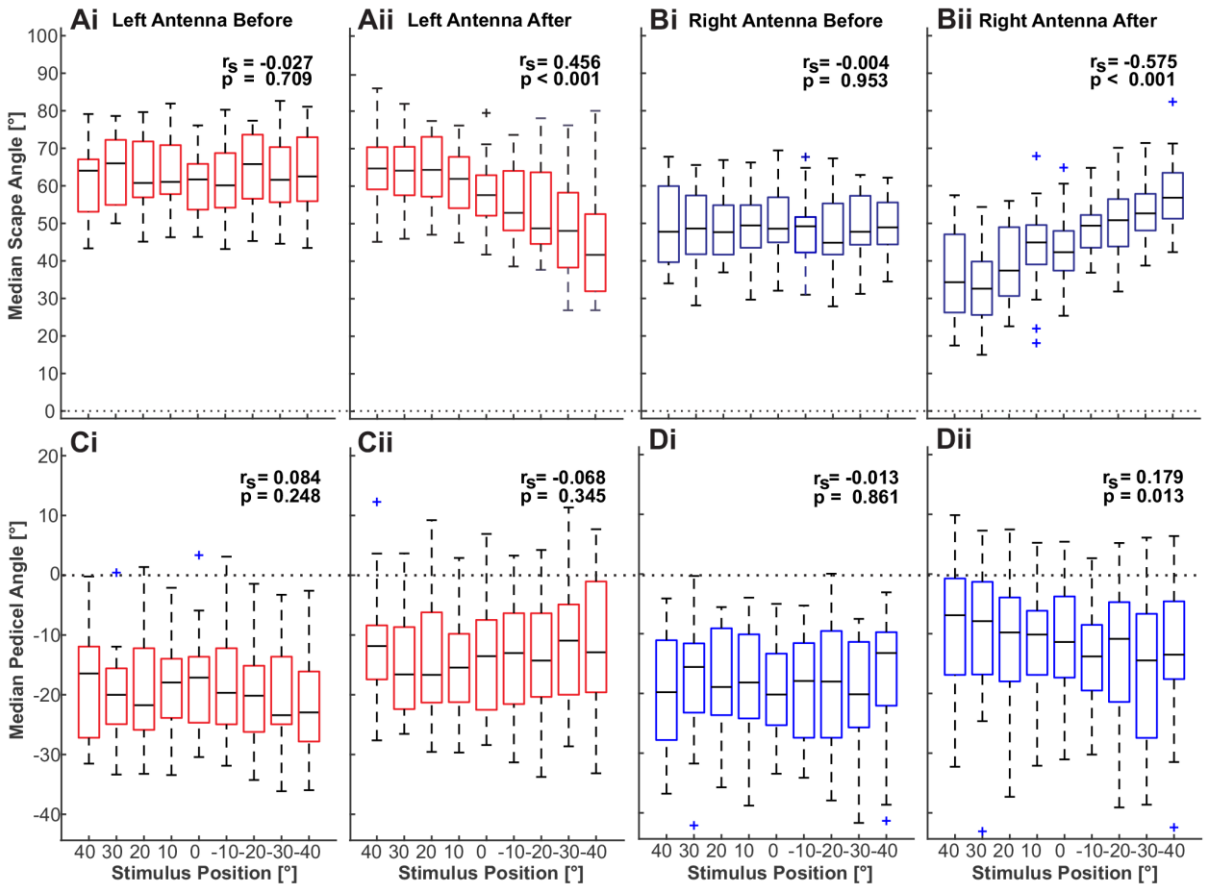

Figure 8: Antennation of the rod is governed by systematic, position-dependent changes of the head-scape, but not scape-pedicel joint angle. A, B) Median angle of the head-scape joint of the left (panels A, in red) and right antenna (panels B, in blue) during walking episodes before (Ai and Bi) and after (Aii and Bii) first antennal contact. C, D) Median angle of the scape-pedicel joint of the left (panels C, in red) and right antenna (panels D, in blue) during walking episodes before (Ci and Di) and after (Cii and Dii) first antennal contact. Box plots show distributions of per-animal means. Numbers of animals and trials in Table 1 B. r_S and p values correspond to Spearman's rank correlation.

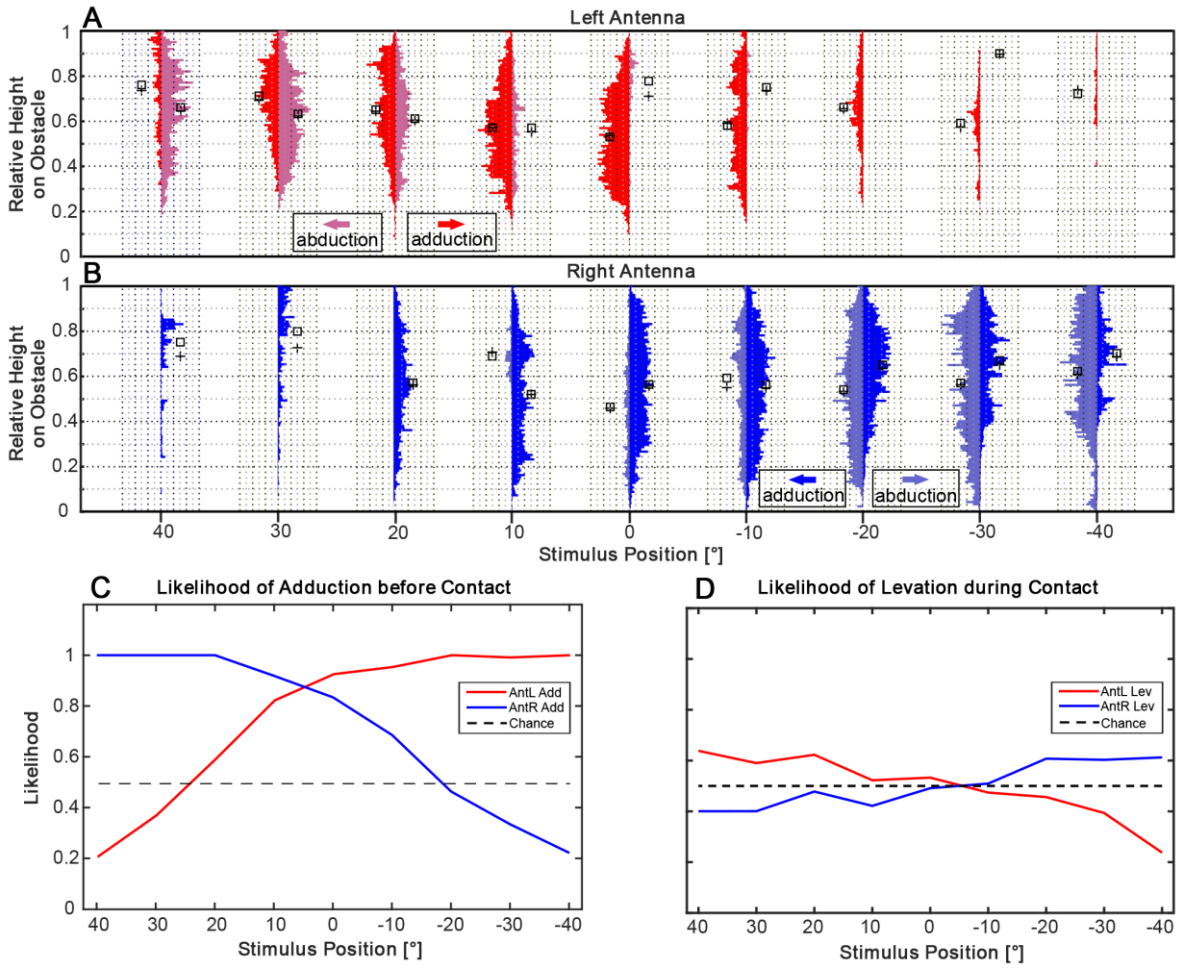

Figure *9*: Both antennae explore the rod at all stimulus positions, with position dependent antennation pattern. A, B) Contacts of either antenna were more frequent if the stimulus was presented on the respective ipsilateral side. Vertical histograms show the mean per-trial distribution of antennal contact location along the rod for left (A, in red) and right (B, in blue) antenna. Laterally directed contacts (following abduction) are shown in lighter colors, medially directed contacts (following adduction) are shown in darker colors. Black squares and crosses indicate median and mean values of the distributions, respectively. Vertical dashed lines indicate steps of 10 frames in the histograms. C): Likelihood of adduction immediately before an antennal contact event. Contralateral contacts (AntR touches left objects or AntL touches right objects) always occur after adduction. D): Likelihood of levation during an antennal contact event: Likelihood of levation is exceeds 50 % for ipsilateral contacts and decreases with increasingly contralateral contact position. For numbers of animals and trials see Table 1 B.

Table 1: Numbers of animals and trials. (A) All trials with at least one antennal contact during the 5 s stimulus presentation. (B) Trials with antennal but no leg contact on the rod. (C) Trials with both antennal and leg contacts on the rod. N_{all} refers to the number of Animals of which Trials for all stimulus positions could be obtained.

Criterion	**Sample sizes**	**Stimulus position**									
		40°	**30°**	**20°**	**10°**	**0°**	**-10°**	**-20°**	**-30°**	**-40°**	**N_{all}**
(A) All, antennal contact	N (animals)	21	25	24	25	25	24	25	24	23	**18**
	n (trials)	58	78	93	95	89	89	90	75	70	
(B) Antennal contact only	N (animals)	17	22	22	24	24	23	23	21	17	**8**
	n (trials)	30	55	79	78	80	80	71	52	37	
(C) Both antennal and leg contact	N (animals)	11	11	6	9	6	6	12	12	14	**2**
	n (trials)	28	23	14	17	9	9	19	23	33	

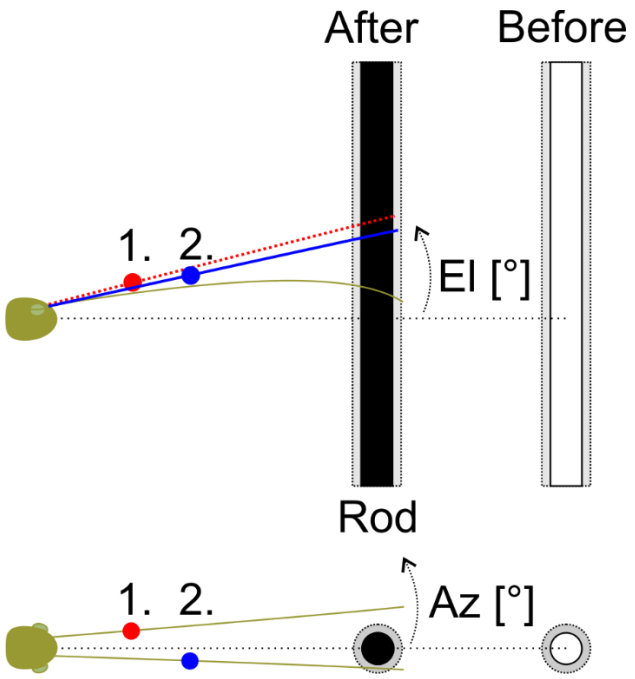

Fig. S1. Antennal contact estimation. Top and bottom panels show schematic side and top views of the experimental situation, respectively. All sizes and distances are drawn to scale. For simplicity, the vertical rod is shown at the central stimulus position (azimuth 0°), before (shaded) and after (solid) being moved into the antennal working-range. Elevation (El [°]) and azimuth (Az [°]) angles are indicated in side and top view, respectively. For motion capture of antennal movement, retro-reflective markers were placed on the proximal third of either flagellum, with the left marker (red) always being placed more proximally than the right marker (blue). Different distances improved tracking reliability but introduced an asymmetry in the estimate of the antennal elevation angles. Dotted red and solid blue lines in the side view show the linear approximation of the left and right antenna, respectively. The linear approximation neglects the slight downward curvature of the distal flagellum. Assuming the same elevation angle for both antennae, a systematic offset in the estimated elevation angle occurred, being larger for the left antenna. Accordingly, estimated antennal contact locations have a systematic upward bias. Note that this vertical bias did not affect the contact detection with the vertical rod. Antennal contacts were detected whenever the antennal azimuth was in the range filled by the rod plus a circular threshold environment (grey zones in schematic). Since markers were always placed on the dorsal surface of the flagellum, the azimuth estimates of the antennae were not biased.

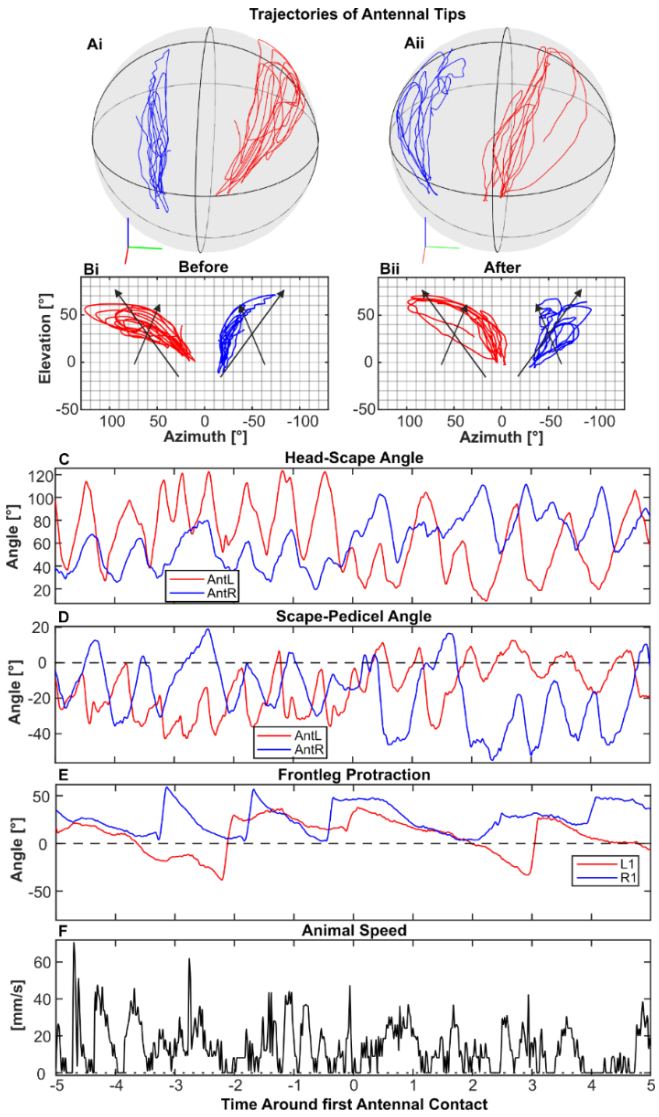

Fig. S2. Antennal movement analysis and additional measurements not used in this study. Same trial as in Fig. 2. A) Tip trajectories of the left (red) and right (blue) antenna, projected on a sphere, 5 s before (Ai) and after (Aii) the first contact event (time 0 in time courses). B) Corresponding azimuth and elevation projection of left (red) and right (blue) antennal pointing direction for the same 5 s episodes as for the spherical trajectories above. Note that the histograms in Fig. 6 and Suppl. Fig. S4 were calculated from single trial data like this. The black arrows illustrate the approximate movement directions of the antennal head-scape (arrows pointing dorso-laterally) and scape-pedicel joints (arrows pointing dorso-medially). C, D) Given the known joint axis orientations of *C. morosus,* both the head-scape joint angles (C) and the scape-pedicel joint angles (D) can be calculated by inverse kinematics (Krause and Dürr, 2004). Note how after the first antennal contact event (time > 0 s) the scape-pedicel time courses of the left (red) and right antenna shift to lower and higher values, respectively (C), corresponding to a ventro-medial shift of the left (red) and a dorso-lateral shift of the right (blue) trajectories between Bi and Bii. Similarly, the relative upward and downward shifts of the left (red) and right (blue) scape-pedicel joint angles in D correspond to dorso-medial and ventro-lateral shifts of the left (red) and right (blue) antennal trajectories, respectively (Bi and Bii). E, F) Further measured variables that were not used in the present paper include the protraction/retraction movements of the left (L1, red) and right (R1, blue) front legs (E), and the translational speed of the animal (F).

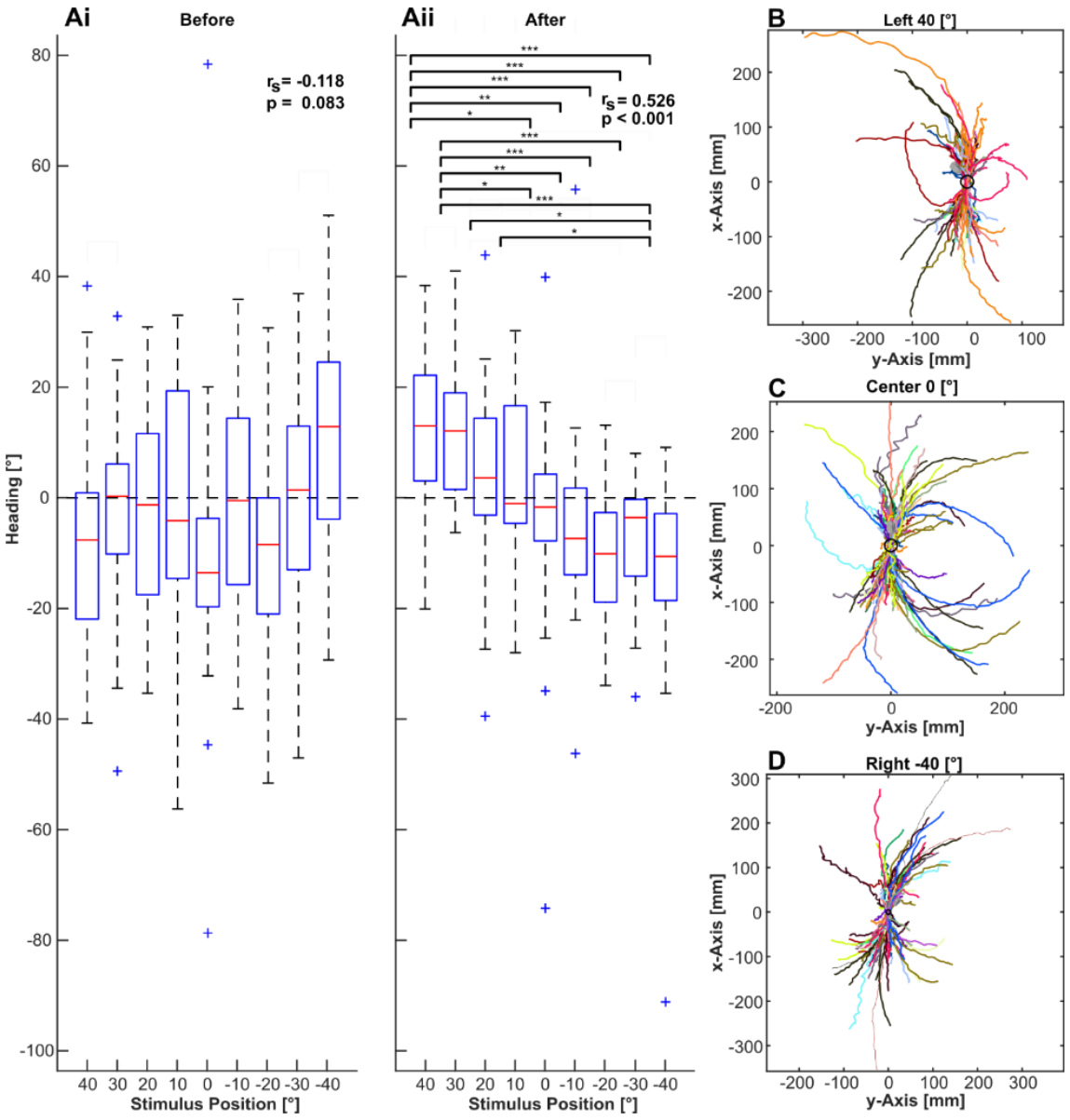

Fig. S3. Animals turn towards the tactile stimulus. Same analysis and graph details as in Fig. 5 but for the entire dataset, i.e., including trials in which the animals grasped the rod with a front leg. The overall similarity with Fig. 5 indicates that the exclusion of leg-contact trials does not affect any conclusion made. (Ai andAii) Mean heading during walking episodes before (Ai) and after (Aii) first antennal contact with the rod. Box plots show distributions of per-animal means. Numbers of animals and trials in Table 1 B. r_S and p values correspond to a Spearman rank correlation. Pair-wise significance levels show results of a post-hoc analysis following a Kruskal-Wallis test (* p <0.05; ** p < 0.01; *** p<0.001). B-D) Animal walking trajectories, shown for all trials of the stimulus conditions -40 °, 0 ° and 40 °. Different colors indicate different animals. Trajectories were centered on the position where the first antennal contact with the rod occurred (black circle) and rotated such that their heading was 0 degrees at this position. Hence the lower and upper parts of the plots show the trajectories before and after fist antennal contact, respectively.

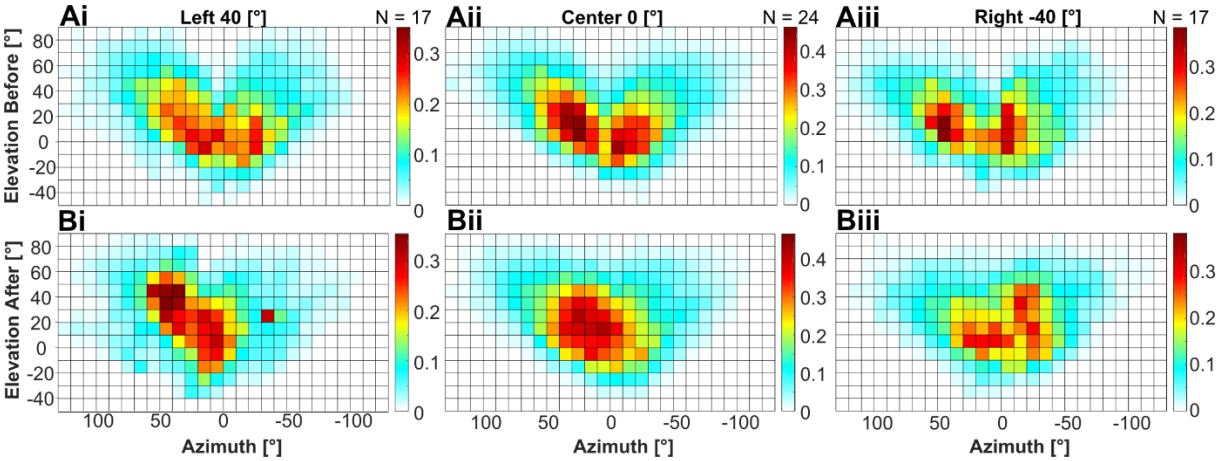

Fig. S4. Active exploration range of the antennae shifts towards stimulus location. Other than Fig. 6, these color-coded maps show antennal azimuth and elevation relative to the prothorax, thus including head movement. A, (top row): before and B (bottom row) after first antennal contact with the rod. Data are averages of normalized per-animal histograms. N gives the number of animals.

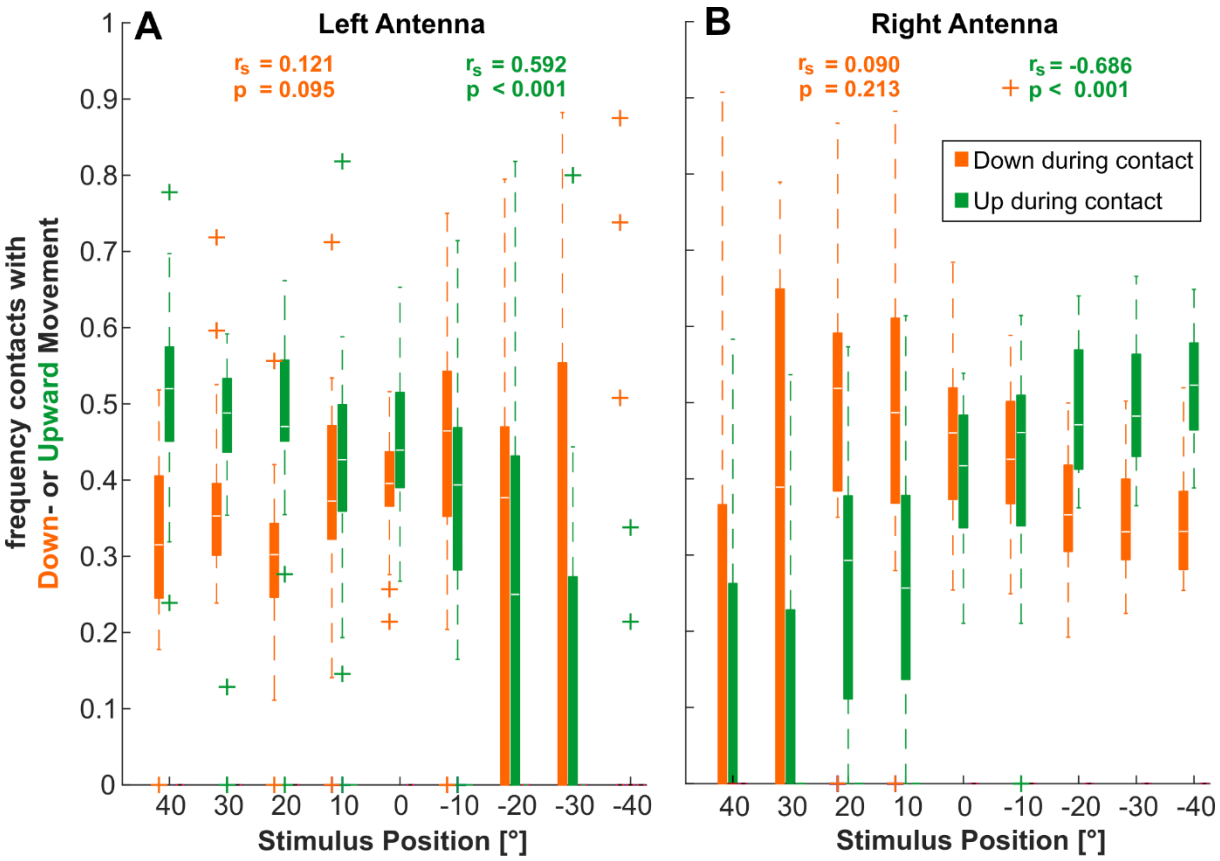

Fig. S5. Antennal movement during contact depends on stimulus position. Boxplots show the relative frequency of downward- (orange) and upward (green) movement during contact events. Relative frequency of upward movement increases with increasingly ipsilateral contact locations, whereas that of downwards movement is highest for contralateral contact locations. r_S and p values correspond to Spearman's rank correlation. For numbers of animals and trials see Table 1 (B).

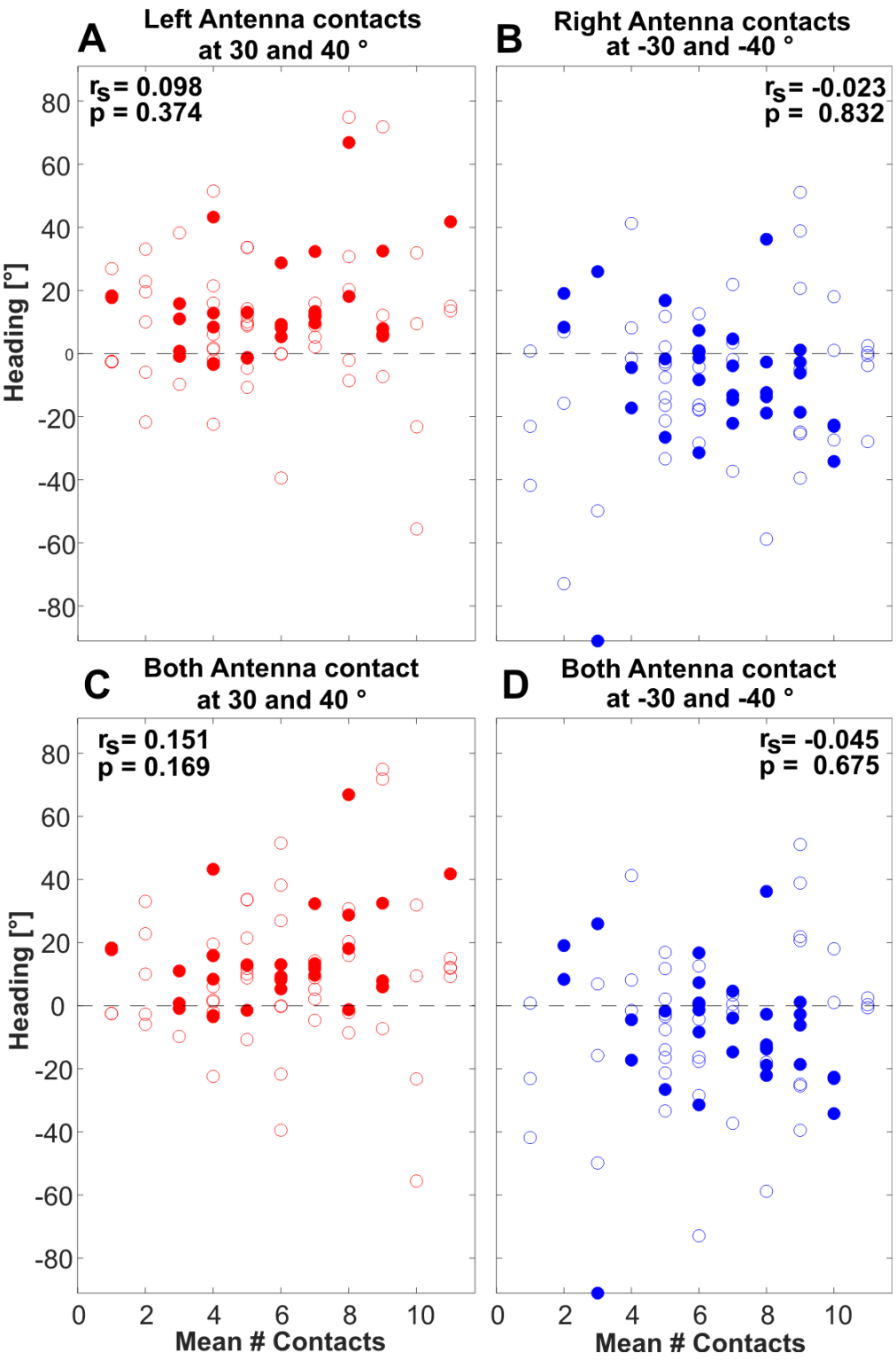

Fig. S6. Change in heading does not correlate with number of Antennal contacts during a Trial. Plots show per Trial number of Antennal contacts on the x axis and heading change on the y-Axis. Values in A are for rod contacts of the left Antenna at the most ipsilateral Stimulus positions 30°(red open circles) and 40° (red filled circles). Values in B are for rod contacts of the right antenna at most ipsilateral Stimulus positions of-30 (blue open circles) and -40° (blue filled circles). Panels C and D show the same than A and B, but for the sum of both antennal contacts. None of the panels shows a significant correlation between number of antennal contacts and amount of change in heading. r_S and p values correspond to Spearman's rank correlation. For numbers of animals and trials see Table 1 (B).